

**Polyanilino-Graphene Oxide Intercalated with Platinum Group Metal  
Nanocomposites, for Application as Novel Supercapacitor Materials**



**UNIVERSITY of the  
WESTERN CAPE**

By

**Nomxolisi Dywili**

(BSc Honours)

A mini-thesis submitted in partial fulfilment of the requirements for the degree of

**Magister Scientiae in Nanoscience**

Faculty of Science

University of the Western Cape

Bellville, Cape Town, South Africa

**Supervisor:** Prof. Emmanuel I. Iwuoha

**Co-supervisor:** Dr C. Ikpo

December, 2014

## ABSTRACT

Supercapacitors are one of the important subjects concerning energy storage which has proven to be a challenge in this country. Currently, the electrodes of most commercial supercapacitors are made of carbon which is known to be inexpensive and has high resistance to corrosion. These carbon based supercapacitors operate under EDLC. They offer fast charging/discharging rates and have the ability to sustain millions of cycles without degrading. With their high power densities, they bridge the gap between batteries which offer high energy densities but are slow in charging/discharging and conventional dielectric capacitors which are very fast but having very low energy densities. The objective of this work was to develop a high performance supercapacitor using polyanilino-graphene oxide intercalated with platinum group metal nanocomposites. Specific capacitance of each material was investigated with the objective of ascertaining the material that has the best capacitance. In this work, GO was functionalized with aniline and intercalated with Pt, Pd and Pd-Pt nanocomposites. The nanomaterials were characterized with FTIR, Ultraviolet-visible (UV-visible) spectroscopy, high resolution scanning electron microscopy (HRSEM), high resolution transmission electron microscopy (HRTEM), energy dispersive x-ray microanalysis (EDS) and X-ray diffraction (XRD) analysis. The composites were tested for possible application as supercapacitor materials using potentiostatic-galvanostatic constant current charge/discharge. The synthesized materials had good electronic, mechanical, optical, physical etc. properties as proven by the various characterization techniques but they proved not to be ideal for application as supercapacitor materials. The materials tested negative when tested for both anodic and cathodic materials therefore we can conclude that the materials are not good supercapacitor materials and therefore cannot be used in application as novel as supercapacitors.

## KEYWORDS

Supercapacitors

Graphene oxide

Aniline

Palladium nanoparticles

Platinum nanoparticles

Palladium-platinum nanocomposites

Electrolytes

Specific discharge capacitance

Specific charge capacitance



## DECLARATION

I declare that “**Polyanilino-graphene oxide intercalated with platinum group metal nanocomposites for application as novel as supercapacitors**” is my own work and that it has not been submitted for any degree or examination in any other university, and that all the sources that I have used or quoted have been indicated and acknowledged by complete references.



Nomxolisi Dywili

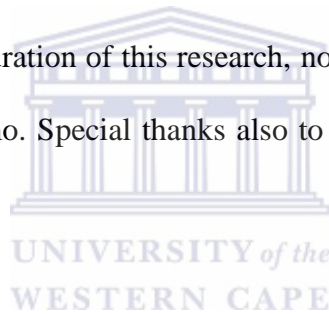
Signed.....

## ACKNOWLEDGEMENTS

My first gratitude goes to the Almighty God. Without him I wouldn't be where I am today in my life. May His Grace and light continue to shine upon us.

Greatest appreciation goes to my parents Mr and Mrs Mankayi for their unconditional love and support throughout my life not forgetting the rest of the family members that put up with me during the sleepless nights and tears

Special thanks to my supervisor Prof Emmanuel Iwuoha for his guidance, support and encouragement throughout the duration of this research, not forgetting the co-supervisors Dr. Chinwe Ikpo and Dr Njagi Njomo. Special thanks also to Dr Julian Key for assisting in the testing of the materials.



Last but not least, a warm thanks to my colleagues. Thank you for your guidance, friendliness and encouragement. Guys, I will never forget you.

## DEDICATION

This work is dedicated to the most important people in my life; Nosipo Mankayi and Bonisile Mankayi and Luxolise Dywili.



## TABLE OF CONTENTS

<b>ABSTRACT.....</b>	<b>ii</b>
<b>DECLARATION.....</b>	<b>iv</b>
<b>ACKNOWLEDGEMENTS .....</b>	<b>v</b>
<b>DEDICATION.....</b>	<b>vi</b>
<b>List of abbreviations .....</b>	<b>x</b>
<b>List of figures.....</b>	<b>xi</b>
<b>List of tables.....</b>	<b>xiii</b>
<b>Chapter 1 .....</b>	<b>1</b>
<b>INTRODUCTION.....</b>	<b>1</b>
1.1 Summary: .....	1
1.2 Research Background .....	1
1.3 Rationale and motivation .....	5
1.4 Objectives .....	6
1.5 Research Framework.....	7
1.6 Investigation outline.....	8
1.6.1 Chapter 2: Literature review .....	8
1.6.2 Chapter 3: Materials and methods.....	8
1.6.3 Chapter 4: Results and discussion.....	8
1.6.4 Chapter 5: Conclusions .....	8
<b>Chapter 2 .....</b>	<b>9</b>
<b>LITERATURE REVIEW .....</b>	<b>9</b>
2.1 Summary .....	9
2.2 Introduction.....	9
2.3 Charge generation and storage in electrochemical capacitors .....	15
2.4 Graphene oxide .....	18
2.4.1 Synthesis of graphene oxide .....	26

2.5	Platinum group metal nanoparticles.....	28
<b>Chapter 3 .....</b>		<b>31</b>
<b>EXPERIMENTAL METHODS .....</b>		<b>31</b>
3.1	Summary .....	31
3.2	Reagents .....	31
3.3	Instrumentation .....	31
3.4	Spectroscopic techniques .....	33
3.4.1	Fourier Transforms Infrared Spectroscopy .....	33
3.4.2	UV-visible spectroscopy .....	34
3.5	Microscopic techniques.....	35
3.5.1	High resolution scanning microscopy .....	35
3.5.2	High resolution transmission electron microscopy .....	35
3.5.3	Energy dispersive spectroscopy .....	36
3.6	X-ray diffraction .....	36
3.7	Electrochemical techniques.....	37
3.7.1	Galvanostatic charge/discharge technique .....	37
3.8	Experimental synthesis .....	39
3.8.1	Synthesis of graphene oxide using the Hummers method .....	39
3.8.2	Functionalization of graphene.....	39
3.8.3	Synthesis of PVP-palladium nanoparticles .....	39
3.8.4	Single step loading of metal nanoparticles on functionalized graphene oxide .....	40
3.8.4.1	Single step reduction of ionic platinum on functionalized graphene oxide .....	40
3.8.4.2	Single step reduction of palladium nanoparticles on functionalized graphene oxide ...	40
3.8.4.3	Single step reduction of palladium-platinum nanocomposites on .....	41
	functionalized graphene oxide .....	41
3.8.5	Fabrication of the electrode material.....	41
3.8.5.1	Preparation of the electrode materials.....	41



3.8.5.2	Construction of supercapacitor cell.....	42
3.9	Overview of main points.....	43
<b>RESULTS AND DISCUSSION .....</b>		<b>44</b>
4.1	Summary .....	44
4.2	The Fourier Transform Infrared Spectrum of GO and f-GO .....	44
4.3	UV-visible spectroscopy .....	46
4.4	High Resolution Scanning electron microscope .....	48
4.5	High Resolution Tunneling Electron Microscopy .....	51
4.6	Energy dispersive spectroscopy .....	52
4.7	X-ray diffraction (XRD) .....	54
4.8	Galvanostatic charge/discharge test .....	56
4.8.1	Testing carbon black as a supercapacitor material.....	56
4.8.2	Testing functionalized graphene oxide as a supercapacitor material .....	59
<b>Chapter 5 .....</b>		<b>63</b>
<b>CONCLUSIONS AND RECOMMENDATIONS.....</b>		<b>63</b>
5.1	Future works and recommendations .....	65
<b>REFERENCES.....</b>		<b>66</b>

## List of abbreviations

GO	Graphene oxide
PGM	Platinum group metals
FGO	Functionalized graphene oxide
EDLC	Electrochemical double layer capacitors
HRSEM	High resolution scanning electron microscopy
HRTEM	High resolution tunneling electron microscopy
XRD	X-ray diffraction
NP	Nanoparticles
CNT	Carbon nanotubes
PANI	Polyaniline
GNS	Graphene nanosheets
GOS	Graphene oxide sheet
EDS	Energy Dispersive Spectroscopy
TMAH	Tetramethylammonium hydroxide



## List of figures

Figure 1: Typical schematic representation of the main elements of a supercapacitor.

Figure 2. Ragone plot

Figure 3. A formation route to anchor platinum (Pt) nanoparticles onto functionalized graphene oxide

Figure 4. Schematic illustration of graphene oxide.

Figure 5. Schematic illustration of GO-based electrodes for electrochemical applications

Figure 6. Number of publications on graphene and graphene oxide in past 20 years

Figure 7: The battery testing unit equipment connected to the monitor

Figure 8. FTIR spectrum of GO and f-GO

Figure 9: UV-vis absorbance spectrum of GO

Figure 10: UV-vis absorbance spectrum of GO and f-GO

Figure 11: SEM image of GO

Fig 12: SEM images of a. f-GO, b. f-GO-Pd, c. f-GO-Pt, d. f-GO-Pd-Pt

Figure 13. TEM images of a. GO and b. FGO

Figure 14: EDS spectroscopy of a. GO, b. FGO and c. FGO-P-Pt nanocomposite

Figure 15: X-ray powder diffraction (XRD) patterns of FGO, FGO-Pd, FGO-Pt and FGO-Pd-Pt

Figure 16a. Cycling plot of carbon black cycled in the anode (negative electrode)

Figure 16b. Cycling plot of carbon black cycled in the cathode (positive electrode)

Figure 17a. Cycling plot of functionalized graphene oxide cycled in the anode (negative electrode)

Figure 17b. Cycling plot of functionalized graphene oxide cycled in the cathode (positive electrode)



## List of tables

Table 1: Overview of specific capacitance and power outputs of a range of graphene based materials and various other comparable materials for use as supercapacitors

Table 2: The parameters used for charge/discharge test

Table 3. Table showing the frequencies and the bonds found in graphene oxide and functionalized graphene oxide

Table 4: Elemental compositions study obtained with EDS

Table 5: Capacitance values of the different materials



## Chapter 1

---

### INTRODUCTION

#### 1.1 Summary:

This chapter deals with the research background whereby supercapacitors and their brief history are introduced. The materials used in the work are also introduced followed by a discussion on the rationale and motivation of the work carried out. The objectives of this work are stated. The research framework and investigations are also outlined in this chapter.

#### 1.2 Research Background

For the past few years the world has faced an energy crisis with predictions that by 2050 the population of the world would have increased to 9 billion, significantly increasing the demand in energy, with oil and natural gas becoming so expensive that they will no longer be sold and used as fuels. North America and the Middle East have been identified as the leaders in energy consumption in the form of burning fossil fuels. It has been proven that the burning of fossil fuels has resulted in the increase of carbon dioxide, methane and other greenhouse gases [1]. The World Energy Outlook (WEO2007) published in 2007 by the International Energy Agency, projected a constant growth in the demand of energy that would, by 2030, require 55% more energy than today. On the other hand, 86% of the actual energy demand is now met with fossil fuels [2]. Energy consumption use is proportional to material capital (consume constant). This relationship has been made constant, since it is not very clear whether it tends to increase or decrease. On one hand technological improvements tend to make a society more efficient in the use of energy but, on the other hand, when the energy available decreases it is more difficult to find good materials for sophisticated energy technologies and the efficiency of these energy production technologies. To help in this energy crisis researchers are looking for ways to improve energy conservation and maximum

energy storage technologies. Much interest has and is being put into energy storage technologies such as batteries, fuel cells and supercapacitors.

Supercapacitors, also known as ultracapacitors or electrochemical capacitors are energy storage devices that employ high surface area electrode materials and thin electrolytic dielectrics to achieve greater capacitances when compared to other energy storage devices such as batteries, fuel cells and conventional capacitors [3, 4]. Batteries are known to maximize the efficiency of energy use. Model electrodes for battery application should be cheap, nontoxic, have high energy and power densities and last long. However, shelf-life and cycle life has proven to be a problem for batteries unlike supercapacitors. Supercapacitors have the ability to maintain a greater shelf-life and longer cycle life with their higher power densities, making them the perfect alternative to batteries [3, 5]. The electrochemical capacitor is an electrical energy storage device that has two electrodes immersed in an electrolyte with a separator between the electrodes (figure 1) much like a battery [3]. The electrodes are known to be fabricated from high surface area, porous material having pores of diameter in the nanometer range. The surface area of the electrode materials used in these capacitors is large, being in the range 500-2000 m<sup>2</sup>/g [3, 5]. Charge is stored in the micropores at or near the interface between the solid electrode material and the electrolyte. Capacitance of a supercapacitor has proven to be a complication when calculated as it depends on complex phenomena occurring at the electrolyte/solid interface of the micropores of the electrode [3, 5]. Capacitance stored is directly proportional to surface area,  $A$  of one plate and inversely proportional to the distance,  $\delta$  of separation between the two plates and is given by:

$$C = \varepsilon \frac{A}{\delta} \quad (1)$$

Wherein,  $\epsilon$ , is known as the dielectric constant (or “permittivity”) of free space. The two attributes of a supercapacitor are its energy and power. The energy,  $E$  stored in a capacitor is directly proportional to its capacitance,  $C$  and is also a factor of potential difference,  $V$ .

$$E = \frac{1}{2}QV = \frac{1}{2}CV^2 \quad (2)$$

The power,  $P$  is the energy expended per unit time. To determine the power of a supercapacitor one must consider the fact that they are represented as circuits in series with external resistance  $R$  in which external components of a supercapacitor e.g. current collector, electrodes and dielectric material, has a high contribution to the resistance and the measured power is given as follows

$$P_{\max} = \frac{V^2}{4R} = I^2R \quad (3)$$

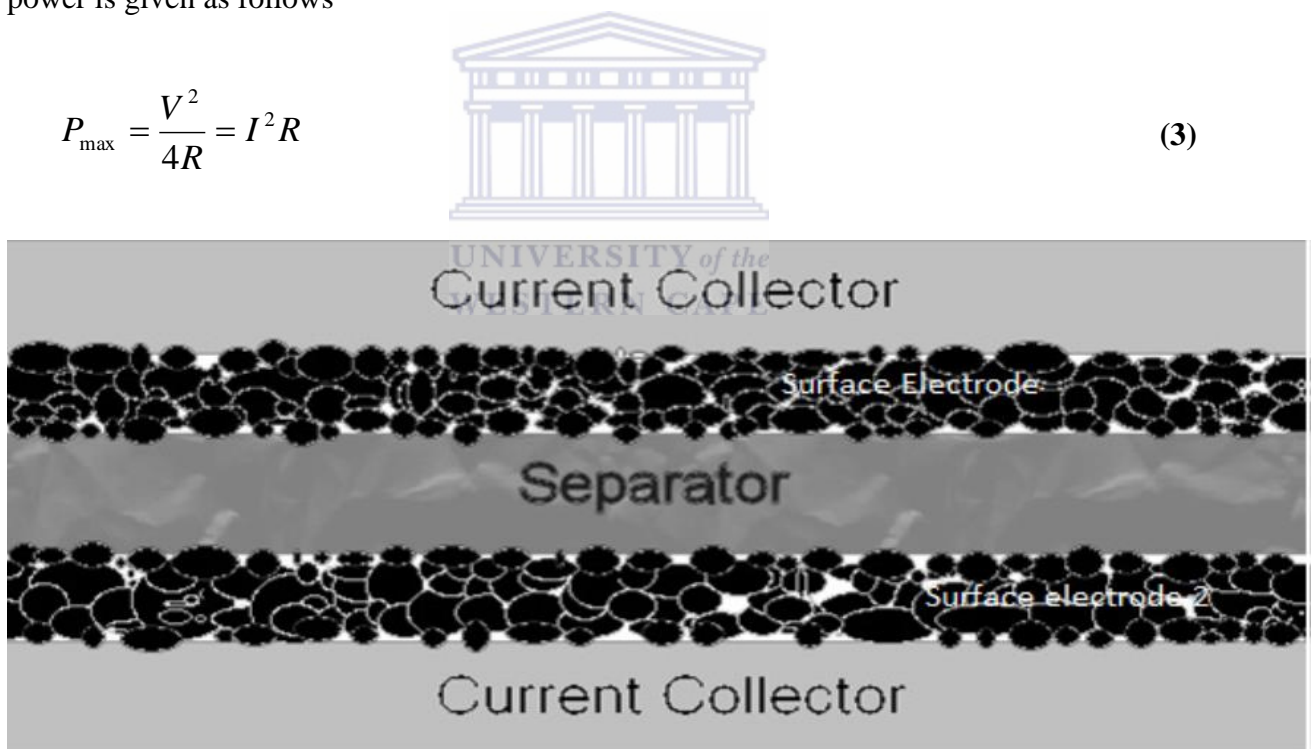


**Figure 1: Typical schematic representation of the main elements of a supercapacitor**

The performance of supercapacitors compared to conventional capacitors, batteries and fuel cells is demonstrated using a Ragone plot [4] given in figure 2. The Ragone plot demonstrates that supercapacitors have higher specific energy than conventional capacitors, but much



lower specific power as compared to them. It also demonstrates that supercapacitors have less specific energy compared to batteries and fuel cells, but attain higher specific power.

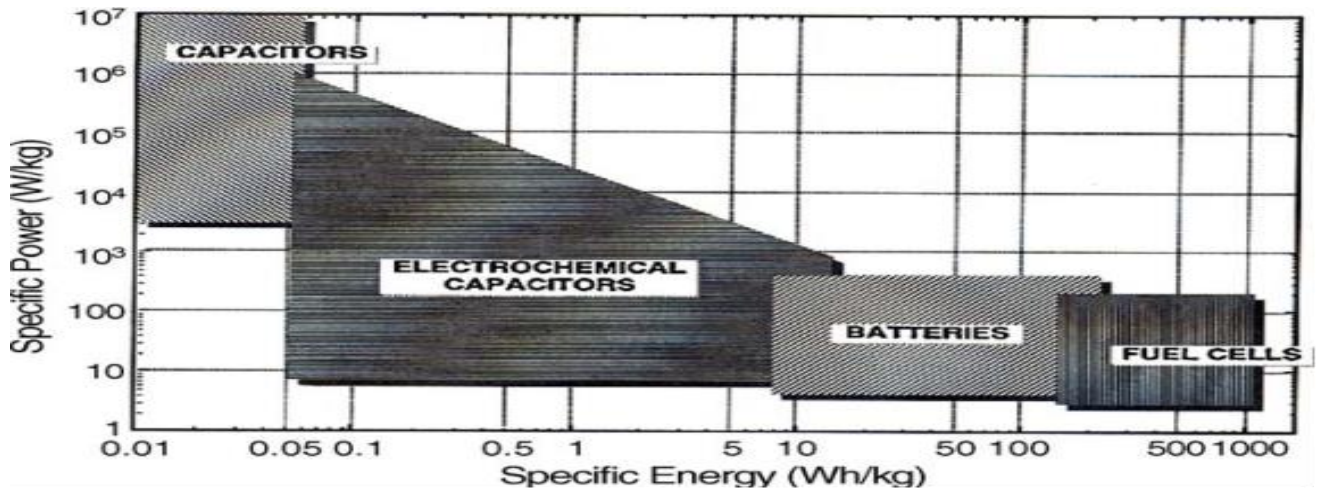
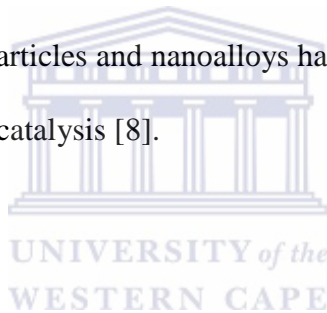


**Figure 2: Ragone plot [14]**

Supercapacitors can be divided into three general classes: electrochemical double-layer capacitors, pseudocapacitors, and hybrid capacitors. Each class is characterized by its unique mechanism for storing charge [6]. These are respectively, non-Faradaic, Faradaic, and a combination of the two. Faradaic processes, such as oxidation-reduction reactions involve the transfer of charge between electrode and electrolyte. A non-Faradaic mechanism, by contrast, does not use a chemical mechanism. Rather, charges are distributed on surfaces by physical processes that do not involve the making or breaking of chemical bonds [6]. Supercapacitors have found application in many areas that exploit supercapacitor advantages to provide resourceful solutions to a variety of emerging energy applications, especially applications that require instant power applications. Such advantages are long lifetime, low impedance, rapid charging and discharging, cost effective energy storage, high energy density, low voltage, linear discharge *etcetera*, [7]. Their high power density makes them perfect for the parallel combination with batteries that have high energy density to push against the hybrid energy storage systems. Supercapacitors have found application in computer systems, UPS systems,

power conditioners, welders, inverters, automobile regenerative braking systems, power supplies, power back up in laptops, mobile phones, digital cameras, iPhone and power generators [10].

The main purpose of this work is to develop a high charge storage material that synergistically combines both the characteristics of an EDLC and a pseudocapacitor. The work aims at synthesizing and characterizing the supercapacitive properties of polyanilino-graphene oxide when intercalated with platinum group metal nanocomposites. This is to determine whether a combination of the properties of polyanilino-graphene oxide with the properties of platinum group nanocomposites can give higher capacitance and energy. Platinum group metals are of much interest due to their attractive electronic and physical properties. Platinum group nanoparticles and nanoalloys have been studied extensively due to their incredible properties during catalysis [8].



### **1.3 Rationale and motivation**

Global economic development and prosperity over past and present century has been built on cheap and abundant fossil fuel with contributions of petroleum at 39%, natural gas at 24% and coal at 23%. There is a limited amount of this fossil fuel. It is non-renewable and therefore an energy crisis is facing the global economic and social world. The increasing demand and popularity of automobiles and various portable electronic devices such as laptops, cellphones and cameras has increased the demand for energy storage devices. However, the performance of these portable electronic devices and automobiles depends strongly on the electrode materials and electrolytes employed during the construction of the energy storage devices. Several emerging nanomaterials with desired nanostructures and large surface/interface areas have been developed for applications in energy-related devices.

Supercapacitors have attracted a lot of attention in the past few years due to their impressive properties. They employ high surface area electrode materials and thin electrolytic dielectrics to attain capacitances that are much greater when compared to conventional capacitors. Batteries can store more total energy than capacitors but cannot deliver it very quickly meaning that their power density is low. Capacitors store relatively less energy per unit mass or volume of electrode materials but the electrical energy stored can be discharged rapidly to produce a lot of power making their power density very high. Much research has therefore been put on supercapacitors. This is the main reason why supercapacitors are the main focus of this thesis.

#### **1.4 Objectives**

The general objective of this work is to develop flexible and high performance polymeric polyanilino-graphene oxide impregnated with platinum group metal and bimetallic supercapacitor electrode nanocomposites materials. The combination of the impressive properties of the polyanilino-graphene and the platinum group metal nanocomposites with a hope of obtaining supercapacitors that will give the best capacitance. Specific objectives are to;

1. Synthesize graphene oxide using the Hummers method.
2. Synthesize palladium (Pd), platinum (Pt) and Pt-Pd nanoparticles.
3. Functionalize graphene oxide with aniline.
4. Intercalate the graphene oxide-aniline with Pt, Pd Pt-Pd nanocomposites.
5. Characterize the composite materials using FTIR, CV, Uv-Visible, SEM, TEM, EDS, XRD.

6. Construct and characterize supercapacitor electrodes and cells using potentiostatic-galvanostatic constant current charge-discharge.

### **1.5 Research Framework**

The first task was to identify the best methods and conditions to prepare the graphene oxide. Two batches of graphene oxide were to be synthesized using the same method and conditions to ensure that the graphene oxide had no impurities and to avoid agglomeration. The graphene oxide was then to be functionalized with aniline to enhance the catalytic performance of hybrids (once the platinum and palladium nanoparticles) have been incorporated on the graphene oxide. It also controls the particle size and avoids agglomeration.

The second task was to characterize the physical properties like size and morphologies of graphene oxide and the functionalized graphene oxide using analytical methods. This gives an insight to the electrochemical behavior of the nanostructure and will help to optimize the preparation conditions and to compare the graphene oxide to the graphene oxide-aniline.

The third task was to synthesize palladium nanoparticles/nanocomposites using various synthesis techniques. The prepared nanoparticles and nanocomposites were to be mounted on the graphene oxide-aniline.

The fourth task was to characterize the composite materials using FTIR, UV-Visible, HRSEM, HRTEM, EDS, and XRD.

The last task was to construct and test supercapacitor electrodes and supercapacitor cells using potentiostatic-galvanostatic constant current charge-discharge in 3-electrode cell configurations in aqueous electrolytes.

## **1.6 Investigation outline**

### **1.6.1 Chapter 2: Literature review**

The literature review involves the introduction of supercapacitors i.e. double layer supercapacitors, pseudo capacitive supercapacitors and hybrid supercapacitors. It also involves the main materials used in this work; graphene oxide its unique properties and as a material of supercapacitors. Platinum group metal nanoparticles are also reviewed in this chapter. Supercapacitors have many applications and South Africa just like other countries is making use of them. Therefore, applications of supercapacitors in South Africa have also been included in this review chapter.

### **1.6.2 Chapter 3: Materials and methods**

The main components of this chapter are the synthesis methods employed to obtain the nanomaterials required and the characterization techniques employed to synthesis the materials. It also outlines the type of materials used.

### **1.6.3 Chapter 4: Results and discussion**

This chapter presents and discusses results of the synthesis of graphene oxide and its functionalization with aniline. Results of the synthesis of the platinum group metal nanocomposites are also discussed. This is then followed by discussions of the morphological and electrochemical studies of the materials by SEM, TEM, FTIR, UV-visible, EDS and CV. Lastly, characterization of supercapacitor cells is discussed.

### **1.6.4 Chapter 5: Conclusions**

The thesis is concluded with a brief discussion of the objectives achieved in relation to the study of the graphene oxide, graphene oxide-aniline and their platinum metal composite nanomaterials as supercapacitor electrodes. Recommendations and possible future work is also discussed

## Chapter 2

---

### LITERATURE REVIEW

#### 2.1 Summary

This chapter covers the detailed role of supercapacitors, their advantages over batteries, fuel cells and conventional capacitors. It mentions the materials used for the fabrication of the supercapacitor electrodes, their mechanical, electronic, optical, electrical properties, conductive etc. This chapter also covers the synthesis methods that have been used in literature to produce these materials. We also learn the specific capacitance that these materials give out when they are used in the fabrication of the supercapacitor electrodes.

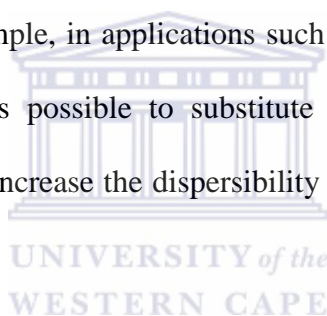


#### 2.2 Introduction

With the global decline in the amount of fossil fuels and the increasing demand in renewable energy, the production, conversion, storage and distribution of this renewable energy have become the main focus of today's world with researchers coming up with attempts to produce efficient and less costly and effective energy storage materials. Supercapacitors, also known as electrochemical capacitors or ultracapacitors, are an important energy storage device owing to its unique power and energy densities range which fills the gap between batteries and traditional capacitors. Typical materials that are known to construct the best supercapacitor electrodes are carbon, conducting polymers and transition metal oxides.

Graphene oxide, a non-conductive hydrophilic carbon material is a good supercapacitor electrode material. First prepared almost 50 years ago, graphene oxide has emerged as a precursor proposing a potential of cost-effective and large-scale production of graphene-based materials [9]. Graphene oxide contains a range of reactive oxygen functional groups

which makes the graphene oxide easily dispersible in water and other organic solvents and this renders it a good candidate for use in many applications [10]. More often graphene oxide is described as an electrical insulator due to the disruption of its  $sp^2$  bonding networks. The reduction of graphene oxide must be achieved, and with it electrical conductivity, in order to recover the honeycomb hexagonal lattice. Once most of the oxygen groups are removed, the reduced graphene oxide obtained is more difficult to disperse due to its tendency to create aggregates and this has to be taken into account [10]. Functionalization of graphene oxide can basically change graphene oxide's properties. The resulting chemically modified graphenes could then potentially become much more adaptable for a lot of applications. There are many ways in which graphene oxide can be functionalized depending on the application on which it is going to be of use. As an example, in applications such as optoelectronics, bio-devices or as a drug-delivery material it is possible to substitute amines for the organic covalent functionalization of graphene to increase the dispersibility of chemically modified graphenes in organic solvents [9, 10].



Recently a platinum hybrid supported by graphene oxide (GO) has attracted attention for its promising potential application in catalysis for fuel cell reactions, sensors and gas storage. GO has been used effectively as a host layered material to prepare hybrids of reduced graphene oxide and metal nanoparticles due to the easy exfoliation and excellent intercalation properties. Graphene oxide could hold small metallic nanoparticles in large quantities loaded uniformly on its surface using aniline as a stabilizer. Functionalizing graphene oxide with aniline stabilizes the reaction of loading the nanoparticles onto the surface of graphene oxide [11]. Combination of graphene oxide and functional nanoparticles have been thoroughly investigated and has been found to lead to materials with interesting properties for a variety of applications, specifically enhancing electrocatalytic activities. Since abundant functional groups on the surfaces of GO can be used as anchoring sites for metal nanoparticles, it is

possible to use them as a support to produce graphene-nanoparticle hybrids [12]. Figure 3 shows the deposition of the platinum nanoparticles onto the surface of functionalized graphene oxide.

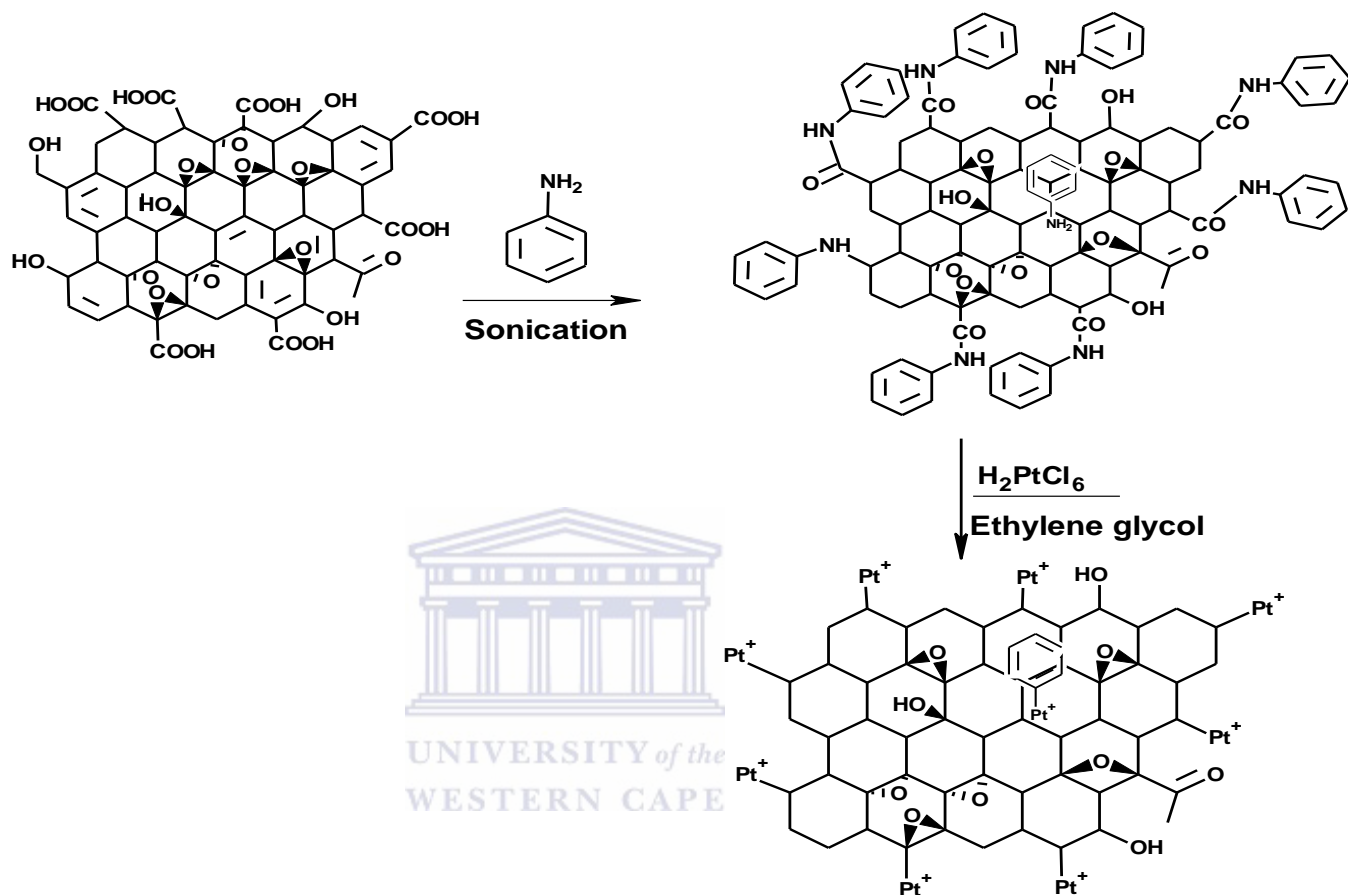


**Figure 3: A formation route to anchor platinum (Pt) nanoparticles onto functionalized graphene oxide**

Composite electrodes incorporate carbon-based materials with either conducting polymer or metal oxide materials, sometimes with a carbon based material such as carbon nanotubes or graphene, and integrate both physical and chemical charge storage mechanisms together in a single electrode [13]. The carbon-based materials enable a capacitive double-layer of charge and also provide a high-surface-area support that increases the contact between the deposited pseudocapacitive materials and electrolyte. The pseudocapacitive materials are able to further increase the capacitance of the composite electrode through Faradaic reactions. Composite



electrodes constructed from combining graphene, polyaniline and metal oxides give a higher capacitance than either pure form of graphene, polyaniline and metal oxides [14]. This combination has been very successful. Other combinations have been tried and tested and they've been observed to give high capacitances [14]. The composites that combine carbon nanotubes with polypyrrole have also been observed to be successful. Several experiments have demonstrated that this electrode is able to achieve higher capacitances than either a pure carbon nanotube or pure polypyrrole polymer-based electrode. This is credited to the accessibility of the entangled mat structure of carbon nanotubes, which allows a steady coating of polypyrrole and a three-dimensional distribution of charge. Furthermore, the structural integrity of the entangled mat has been shown to limit the mechanical stress caused by the insertion and removal of ions in the deposited polypyrrole. Therefore, unlike conducting polymers, these composites have been able to achieve a cycling stability comparable to that of EDLCs [14, 16].

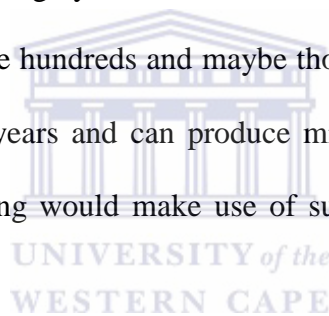
Energy and power are highly dependent on the internal resistance. The two factors are highly dependent upon the conductivity and voltage range of the electrolyte. The two principal factors that are involved in conductance are concentration of free charge carriers (cations and anions) and their ionic mobility or conductance contribution per dissociated ion in the electrolyte [15]. These two factors also have sub-factors that guide them [16]. They are the solubility of the selected salt, degree of dissociation into free ions and factors such as extent of cation-anion association or pairing of ions of the dissolved salt [16, 17]. This in turn is influenced by the salt concentration, temperature and the dielectric constant of the solvent and lastly the viscosity of the solvent, which is a temperature dependent property. As temperature increases, there is a corresponding decrease in viscosity. There is also the necessity for a solvent to be chemically stable as stability is very important when considering

that supercapacitors charge and discharge many times during their operational lifetime [16, 17].

In supercapacitor research, many researchers prefer to use non-aqueous electrolytes for higher operating voltages can be utilized due to the larger decomposition limits of such electrolyte solutions. We get blended electrolytes which contains a solution of a conductive salt dissolved in a solvent. Such common solvents are acetonitrile, sulfolane, propylene carbonate, diethyl carbonate, etc [18]. Gel-polymer electrolytes are also used. These can be classified as a two-phase system composed of ionically conducting medium entrapped in host polymer matrix [18]. The most important ionic conductors are proton ( $H^+$ ) and lithium ( $Li^+$ ) based electrolytes. Gel-polymer electrolytes have many advantages which can be applied in manipulating supercapacitors design architecture, i.e. they can be made of any size, shape and light weight to achieve high energy density without incorporating volatile organic solvents [18]. The use of biodegradable ionic electrolytes meets the environmental challenges while enhancing the potential range of the devices for high energy storage. Increasing the energy density and discharge rates of supercapacitors will enable them to compete with batteries and conventional electrolytic capacitors in a number of applications. Ionic liquid electrolytes involves a family of salts known as hydrophobic ionic liquids which possess a unique set of physical, chemical and electrochemical properties that strongly favor their use as electrolytes in supercapacitors [18]. Their properties include ion concentration from 4M to 6M, wide working temperature range from  $-90^{\circ}C$  to  $400^{\circ}C$ , non-flammability with low toxicity, non-corrosive to electrodes and packing components at elevated temperatures and isothermal stabilities approaching  $300^{\circ} C$  with no measurable vapor pressure. The viscosities are minimally two orders of magnitude greater than those of most common molecular solvents [18]. Typically, ionic conductivity is in the range from 4 to 14 mS/cm at  $22^{\circ}C$ . This

conductivity is insufficient for supercapacitors at room temperature and below, but is suitable for high temperature applications.

South Africa is making use of supercapacitors, especially in coupling them with photo-voltaic (PV) cells. Photo-voltaic street lighting is mainly used in parts of the country where national grid electricity is not available. Street lighting in South Africa accounts for about 24% of the total energy consumed by South African municipalities and contributes approximately 28% of the carbon emitted by municipalities in the delivery of services. It was found that most PV systems use deep cycle batteries for storage which have low efficiencies whereas supercapacitors have high efficiencies ranging between 95-98%. It was also found that PV systems require batteries with a long cycle life but standard batteries have a life expectancy of 2-3 years and can only produce hundreds and maybe thousands of cycles. Supercapacitors have a life expectancy of 7-10 years and can produce millions of cycles. It was therefore decided that the PV street lighting would make use of supercapacitors instead of standard batteries [19, 20].



A company called Murata announced the addition of the DMG series to the company's line of thin, low-resistance, electrical double-layer capacitors (EDLCs). The DMG supercapacitors provide high power back-up. Achieve high reliability with a five-year life span at 70° C, making them an ideal choice for enterprise solid state drive (SSD) manufacturers and telecom “last gasp” applications. Smart meters are also a key application for the DMG series as the full operating temperature range is – 30<sup>0</sup> C to + 85<sup>0</sup> C. This DMG series offers high voltage with very low equivalent series resistance (ESR) all within a miniaturized, yet tough package. Available in 2.1 V single-cell and 4.2 V double-cell options, the 2.1 V provides a nominal capacity of 700 mF with a profile of only 1.4 mm and an ESR at 1 kHz 70. The 4.2 V devices have a nominal capacity of 350 mF at 2.8 mm thickness and 130 ESR at 1 kHz. The DMG series has high capacitance values in a small and low profile design

due to the carbon which is used as an electrode and leads to a longer cycle life. Measuring at only 20.5 mm x 18.5 mm x 1.4 mm, leads the industry in compact packaging. Murata's EDLC series is designed for extended temperature applications. The foundation behind this new technology is the consequence of Murata's partnerships with CAP-XX. In order to meet consumer demand for mobile devices with greater efficiency and functionality, Murata strategically acquired leading edge super cap technology from CAP-XX in 2008. Since then, Murata's focus on EDLC research and development, coupled with CAP-XX's expertise, has led to the maturity of the enhanced EDLC design [18, 19, 20].

### **2.3 Charge generation and storage in electrochemical capacitors**

Electrochemical double-layer capacitors (EDLCs) are constructed from two carbon-based electrodes, an electrolyte, and a separator [21, 22, 23]. Energy storage in EDLC is electrostatic in nature and arises from the separation of electronic and ionic charges at the interface across the double layer of supercapacitor electrodes. There is no transfer of charges across the double layer. EDLCs apply an electrochemical double-layer of charge to store energy. As voltage is applied, charge accumulates on the electrode surfaces [21]. Following the natural attraction of unlike charges, ions in the electrolyte solution diffuse across the separator into the pores of the electrode of opposite charge. However, the electrodes are engineered to prevent the recombination of the ions [21, 23]. Thus, a double-layer of charge is produced at each electrode. These double-layers, coupled with an increase in surface area and a decrease in the distance between electrodes, allow EDLCs to achieve higher energy densities than conventional capacitors [21, 23]. For an electrochemical capacitor energy stored is determined as  $\frac{1}{2}CV^2$ . The capacitance  $C$  is dependent primarily on the characteristics of the electrode material such as surface area and pore size distribution [21,

22]. For an ideal EDLC, the charge is transferred into the double layer and there are no Faradaic reactions between the solid material and the electrolyte [21, 22]. For this reason, charge storage in EDLCs is highly reversible, which allows them to achieve very high cycling stabilities. However, EDLCs suffer from low energy densities [24]. Different forms of carbon materials such as activated carbons, carbon aerogels and carbon nanotubes can be used to store charge in EDLC electrodes. Because activated carbon is less expensive and possesses a higher surface area than other carbon based materials, it is therefore the most commonly used electrode material in EDLCs [21, 22]. There is also an interest in using carbon aerogels as an electrode material for EDLCs as carbon aerogels are formed from a continuous network of conductive carbon nanoparticles with interspersed mesopores. Due to this network and their ability to bond chemically to the current collector, carbon aerogels do not require the use of adhesive binding agent. They therefore have been shown to have a low Equivalent Series Resistance (ESR). Unlike other carbon based electrodes, the mesopores in carbon nanotube electrodes are interconnected, allowing a continuous charge distribution that uses almost all of the available surface area. Thus, the surface area is utilized more efficiently to achieve capacitances comparable to those in activated-carbon-based supercapacitors even though carbon nanotube electrodes have a modest surface area compared to activated carbon electrodes [23, 24, 25]. It has been shown that carbon based materials such as carbon black, graphene, graphite; carbon nanotubes give the best EDLC. Carbon electrode materials generally have higher surface area, lower cost, and more established fabrication techniques than other materials such as conducting polymers and metal oxides [26].

When a solid is immersed partly in an electrolyte, a potential is automatically set up across the two phases i.e. at the electrode/electrolyte interface therefore common terminology in electrochemistry is that a double layer is set up at the interface. The double layer at the interface between two phases has electrical, compositional, and structural characteristics. The

electrical and compositional characteristics deal with the excess charge densities on each phase and the structural one with the distribution of the constituents (ions, electrons, dipoles, and neutral molecules) in the two phases, including the interfacial region [21, 27].

For pseudo-capacitance devices, the charge is mostly transferred at the surface or in the bulk near the surface of the solid electrode material. Therefore, we can conclude that the interaction between the solid material and the electrolyte involves Faradaic reactions. Fast faradaic reactions take place to an extent limited by finite amount of active material or available surface [25]. The charge transferred in these reactions is voltage dependent resulting in pseudo-capacitance also being voltage dependent [23, 25, 26]. Capacitance arises due to progressive redox reactions between several oxidation states [23, 25, 26]. There exist three types of electrochemical processes that have been utilized to assist in the development of supercapacitors that make use of pseudo-capacitance. They are the surface adsorption of ions from the electrolyte, redox reactions involving ions from the electrolyte and the doping and de-doping of active conducting polymer material in the electrode [21]. These first two processes are surface mechanisms and are therefore dependent on the surface area of the electrode material and the last process involves conducting polymers and is more of a bulk process [21]. There are two electrode materials that are used to store charge in pseudocapacitors; conducting polymers and metal oxides [25]. Conducting polymers have a relatively high capacitance and conductivity, plus a relatively low ESR and cost compared to carbon-based electrode materials which makes it a good candidate for pseudo-capacitors. Furthermore, it is believed that the mechanical stress on conducting polymers during reduction-oxidation reactions, limits the stability of these pseudocapacitors to low charge-discharge cycles [25]. It has been shown that transition metal oxides such as nickel oxide, chromium oxide, and copper oxide etc. give the best pseudo-capacitance. The best known metal oxide which gives highest capacitance is ruthenium oxide [26], but due to its scarcity

and high cost other alternatives are being investigated. Some of the oxides which have been studied as pseudo-capacitive electrode materials are NiO, Ni(OH)<sub>2</sub>, MnO<sub>2</sub>, Co<sub>2</sub>O<sub>3</sub>, IrO<sub>2</sub>, FeO, TiO<sub>2</sub>, SnO<sub>2</sub>, V<sub>2</sub>O<sub>5</sub> and MoO [27]. None of these oxides are used in commercial production of EDLCs and they are still in laboratory-scale research.

Hybrid capacitors are ultracapacitors that have been fabricated with one electrode that is of a double-layer i.e. carbon material, and the other electrode being of a pseudo-capacitance material [21]. Most of these hybrid capacitors that have been developed make use of nickel oxide as the pseudo-capacitance material in the positive electrode. We observe a significantly higher value of energy density when comparing the energy density of these devices to those of double layer capacitors. [27, 28, 29]. Hybrid capacitors can also be assembled using two non-similar mixed metal oxides or doped conducting polymers. Hybrid capacitors attempt to exploit the relative advantages and mitigate the relative disadvantages of EDLCs and pseudocapacitors to realize better performance characteristics [29].

#### **2.4 Graphene oxide**

Graphene is a two-dimensional sheet of sp<sup>2</sup>-hybridized carbon and its honeycomb network is known to be the building block of other allotropes, as it can be stacked to form 3D graphite, can be rolled up to form 1D nanotubes, and can be wrapped up to form 0D fullerenes. The long range  $\pi$ -conjugation of graphene gives extraordinary thermal, mechanical and electrical properties [28, 29]. However, graphene is just one sheet of graphite and it is the thinnest strongest material ever isolated with electrical charge carriers moving at speeds 10-100 times faster than in today's silicon chips. Graphene is stable in air, transparent and flexible [30]. Graphene is considered to be the most potential electrical double layer capacitors' material due to its high electrical conductivity, good electrochemical stability, high surface area and superior mechanical property [28, 29]. One specific branch of graphene research, deals with graphene oxide (GO), which is considered to be a precursor for graphene synthesis either by

chemical or thermal reduction. GO is known to consist of a single-layer of graphite oxide and is usually produced by the chemical treatment of graphite through oxidation, with successive dispersion and exfoliation in water or in other suitable organic solvents. Due to its structure, there have been several structural models proposed over the years whereby these adopt the presence of various oxygen containing functional groups in the GO and these oxygen functional groups have been identified as mostly in the form of hydroxyl and epoxy groups with smaller amounts of carboxyl, carbonyl, phenol, lactone, and quinone at the sheet edges [30, 31, 32]. The oxygenated groups in GO are so strong and they can strongly affect the mechanical, electronic and electrochemical properties of graphene oxide. The polar oxygen functional groups of GO give it a strong hydrophilic property which gives the GO high dispersibility in many solvents most particularly in water. Furthermore, these functional groups serve as sites for chemical modification or functionalization of GO which in turn can be used to immobilize numerous electroactive species through covalent or noncovalent bonds for the design of sensitive electrochemical systems [31, 32]. GO can be made into an insulating, semiconducting, or semi-metallic material by fine tuning the oxidation or reduction parameters with a view to controlling the structural disorder. Despite the intense interest and the continuing experimental success by chemists, widespread implementation has yet to occur. This is due to the problem of producing high quality samples in any accessible fashion [32, 33, 34].



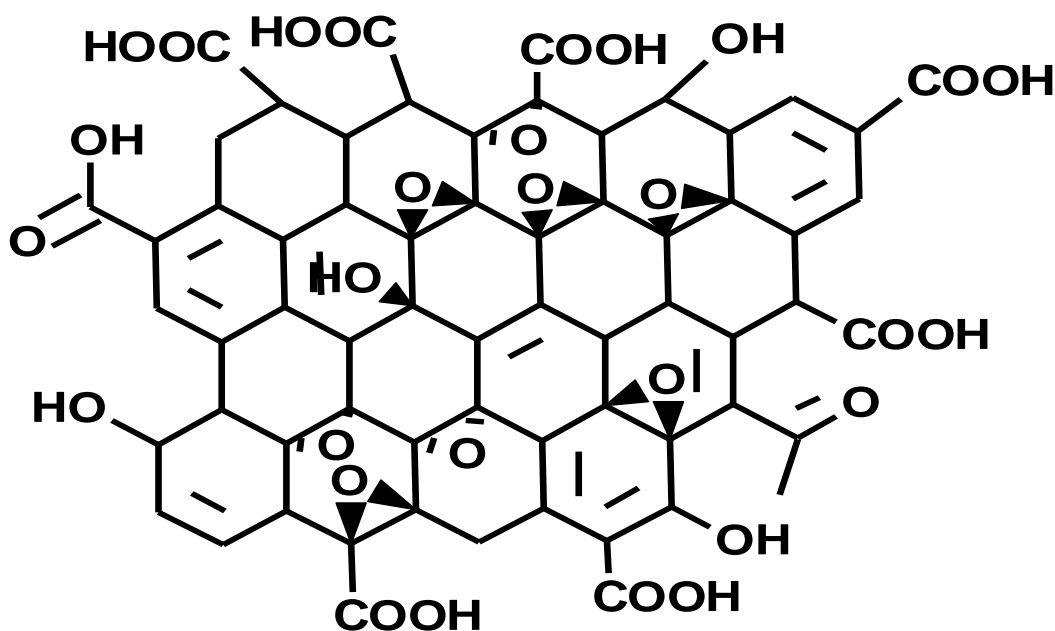


**Figure 4: Schematic illustration of graphene oxide.**

GO based materials have been studied extensively over the years with much interest based on its electrochemical behavior so that it could be applied in electrochemical applications. Sustaining the significance of graphene oxide based materials in electrochemistry are the very specific properties that although relevant to GO are not typical of pristine graphene. These include its facile synthesis, high dispersibility in a range of solvents, capability of coupling electroactive species onto the surface and unique optical properties such as fluorescence labels [35, 36, 37]. Furthermore, the use of GO-based materials also provides control over the local microenvironment because in most cases GO-based materials can be deposited, with extremely well-defined surfaces, through solution processing. This gives graphene oxide an advantage when sensitive and electroactive species are to be incorporated into an electrochemical species. Another important issue to consider is the cost when producing an electrode for application in any real system [38, 39, 40]. In terms of the production of graphene oxide based devices, costs can be reduced compared with the costs for conventional electrodes. This is due to the fact that only a fraction of the amount of GO-based materials is

obligatory for solution processed thin film deposition. Moreover, GO-based thin conductive films deposited onto an inexpensive base material can lead to a larger surface area-to-volume ratio, which further lowers the cost of the electrode [40]. Meanwhile, the large effective surface area can also provide a larger number of active sites and often also a higher signal-to-noise ratio. Owing to these advantageous specific properties, GO-based materials have been used to design and prepare GO-based electrodes for a wide range of applications in electrochemical sensors and electro-analysis as shown in figure 5 [31, 32, 41].

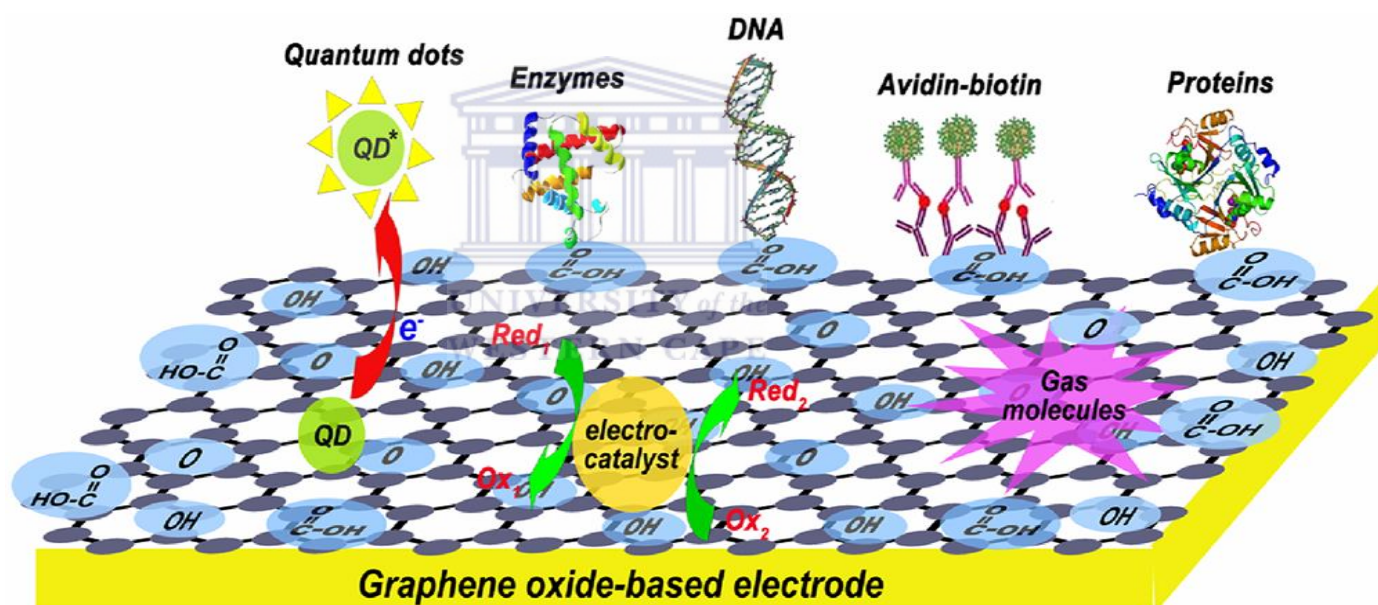


**Figure 5: Schematic illustration of GO-based electrodes for electrochemical applications [32].**

There is no doubt that graphene oxide has risen as a shining star in the horizon on the path of the scientists' search for new materials for future energy, electronic and composite industry. Since the discovery of graphene, the number of publications has increased tremendously as shown in figure 6.

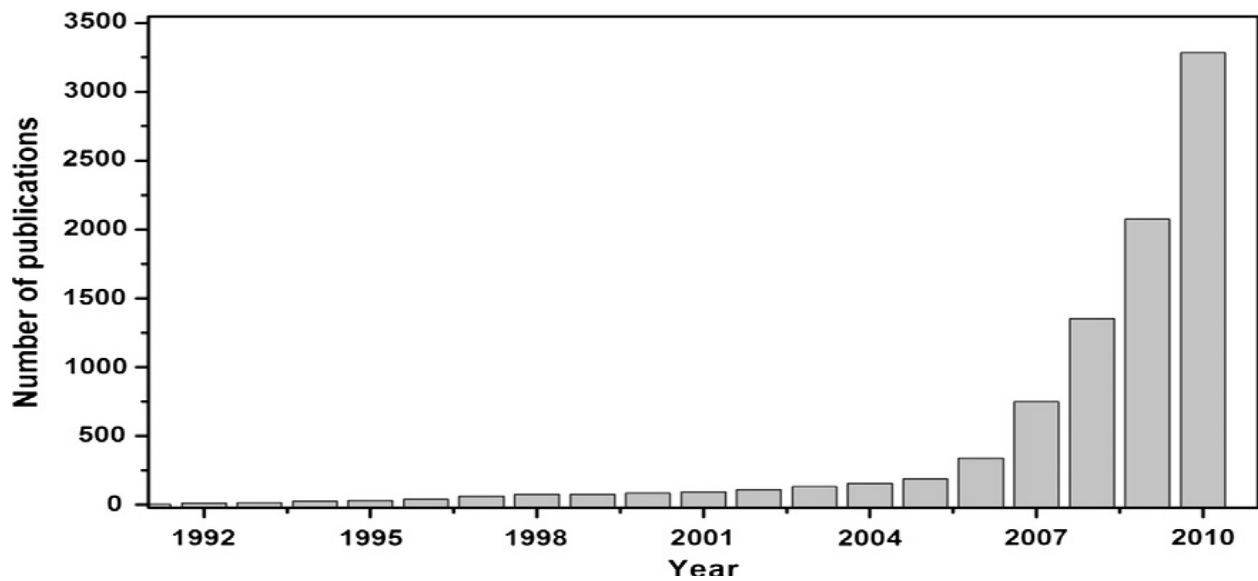


**Figure 6: Number of publications on graphene and graphene oxide in past 20 years.**

The use of graphene as a supercapacitor material has been extensively reported, with many reports reporting that graphene is a superior supercapacitor material compared to carbon and polymer based materials [38, 41]. Table 1 shows a selection of literature reviews in which it is evident that graphene is superior compared to CNTs

**Table 1: Overview of specific capacitance and power outputs of a range of graphene based materials and various other comparable materials for use as supercapacitors [43].**

Electrode material	Performance parameter		Cyclicability	Comments
	Specific capacitance (F g <sup>-1</sup> )	Power density (kW/kg)		
Graphene	205	28.5	~ 90% specific capacitance which remains after 1200 cycles	Graphene was prepared from graphite Oxide
GNS	150	NT	Specific capacitance was maintained with the specific current of 0.1Ag <sup>-1</sup> for 500 cycles of charge/discharge	N/A
PANI	115	NT	NT	Synthesized using in situ polymerization. Capacitance obtained from CV measurement at a SR of 1mVs <sup>-1</sup>
GOS/PANI	531	NT	NT	Nanocomposite with a mass ratio of PANI/graphene, 100:1. Capacitance

				obtained by charge-discharge analysis
--	--	--	--	---------------------------------------

**GNS (graphene nano-sheets); PANI (polyaniline); GOS (graphene oxide sheets); NT (not tested); NA (not applicable)**

According to the energy storage mechanisms depicted above, the tool to improving specific capacitance is to enlarge the specific surface area and control the pore size, layer stacking, and distribution of the electrode material. Graphene was investigated as a potential supercapacitor electrode material; with a maximum specific capacitance of 205 F/g, power density of 10 kW/kg, energy density of 28.5 Wh/kg, excellent cyclicability was obtained with approximately 90% specific capacitance remaining after 1200 cycles. GNS has a specific capacitance of 150 F/g, power density has not been tested and cyclicability was obtained with specific capacitance being maintained after 500 cycles of charge/discharge at specific current of 0.1 A/g. PANI has a specific capacitance of 115 F/g, power density and cyclicability have not been tested. It has been reported that composites of different materials give the best capacitance. This has been shown to be the case with the combination of graphene oxide and polyaniline which have given a specific capacitance of 531 F/g at a mass ratio of 100:1. The values of GNS and PANI for specific capacitance are much smaller when compared to that of graphene [38, 39, 41].

Vivekchand et al. [44] has shown that using an ionic liquid electrolyte to enable the operating voltage to be extended up to 3.5V, graphene prepared via graphitic oxide, exhibits a specific capacitance and energy density of approximately 75 F/g and 31.9 Wh/kg respectively. This exceeds those of both single walled carbon nanotubes (SWCNTs) and multi-walled carbon nanotubes (MWCNTs) whose specific capacitances are 64 and 14 F/g respectively. The writers claim that this value is one of the highest values reported to date, confirming that the

routine features of graphene are related directly to its quality in terms of numbers of graphene layers and inherent surface area [42, 44].

However, it is evident that graphene's general specific capacitance is not as high as expected, and thus many researchers have turned to the integration and fabrication of graphene based hybrid materials in the pursuit for improved capacitance performance [45]. Reports display that composites of graphene oxide with PANI or CNT give the best specific capacitance with values ranging from 216 F/g to 1046 F/g. Further work has indicated that graphene oxide has the potential to outperform its counterparts as a capacitor material; for example it has been underlined that graphene oxide–ZnO composite displays improved capacitances when compared to CNTs, as well as an improved reversible charge/discharging ability [43]. Other work which has been explored shows that when inorganic nanomaterials are anchored on graphene oxide's surface, enhanced specific capacitance is evident [43, 44]. Having overviewed the application of graphene oxide as a supercapacitor material, it is evident that graphene oxide has already made a substantial influence and revealed itself to be a promising material for future energy and supercapacitor research. With the possibility of hybrid graphene oxide materials developing in the near future, we may observe the fabrication of a supercapacitor composite that is able to obtain unachievable capacitance levels and greatly improved cyclic abilities. The only major limitation is the current cost of graphene, its reproducibility, scalability, and characterization. Drawing from the latter, many reports are emerging where claims of utilization of graphene are made without adequate characterization being performed. In such cases perhaps graphene is not present at all, rather multiple layers of graphene. Therefore, suitable control experiments need to be performed where results are compared to other appropriate carbon forms such as graphite or activated carbons.

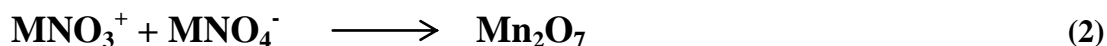
It has been shown that for composites that include carbon based materials such as graphene oxide and pseudo-capacitive materials such as conductive polymers, much capacitance can be

obtained. The functionalization of graphene oxide enhances the capacitance as well as providing anchoring sites for the impregnation of pseudo-capacitive materials such as metal and metal alloy nanoparticles (e.g. platinum group metals and their nanoalloys) and metal oxide nanoparticles or conducting polymers [46, 47]. The use of functionalized graphene as a support for the pseudo-capacitive materials avoids their agglomeration and helps these nanoparticles to achieve maximum utilization of their metal oxide characteristics. It also helps in the growth of nanostructured polymers which helps in achieving high values of capacitance [46]. Present studies reveal that graphene attain a specific capacitance as high as 117 F/g in aqueous sulphuric acid. In the ionic liquid, a specific capacitance of 75 F/g is approximately attained with an energy density of approximately 31.9 Wh/kg [48].



#### **2.4.1 Synthesis of graphene oxide**

The first synthesis of graphene oxide was prepared by the micromechanical cleavage of from highly ordered pyrolytic graphite. In this synthesis method, a layer is peeled off from the graphite using scotch tape and then transferred on to the silicon substrate [49]. The common method mostly used currently to prepare graphene oxide is the simple and modified Hummers method (Graphite,  $H_2SO_4$ ,  $KMnO_4$ ,  $H_2O_2$ ) and ( $KMnO_4$ ,  $NaNO_3$ ,  $H_2SO_4$ ) respectively. The Hummers method [30] uses a combination of potassium permanganate with sulphuric acid. Permanganate is widely used as an oxidant but the active site is the diamanganese heptoxide. The formation of diamanganese heptoxide from potassium permanganate in the presence of a strong acid is as follows:



The simple Hummers method involves treating graphite with potassium permanganate and sulphuric acid, with water added and the whole reaction taking place in an ice bath. This is then followed by the addition of hydrogen peroxide whose function is to stop the gas production that comes out of the reaction. The modified Hummers method involves treating graphite with sodium nitrate and sulphuric acid under constant stirring. After an hour potassium permanganate is added into the reaction keeping the temperature less than 20°C to prevent overheating and the evolution of gases. The mixture is then stirred at 35°C for 12 h and the resulting solution is diluted by adding 500 ml of water under vigorous stirring. To ensure the completion of reaction with  $\text{KMnO}_4$ , the suspension is further treated with 30%  $\text{H}_2\text{O}_2$  solution (5 ml). The resulting mixture is washed with HCl and  $\text{H}_2\text{O}$  respectively, followed by filtration and drying, graphene oxide sheets were thus obtained [50]. Researchers are attempting to come up with better synthesis methods of graphene oxide and Marcano et al has come up with an improved synthesis method of graphene oxide. In their method instead of using the sodium nitrate, increasing the amount of  $\text{KMnO}_4$ , and performing the reaction in a 9:1 mixture of  $\text{H}_2\text{SO}_4/\text{H}_3\text{PO}_4$  improves the efficiency of the oxidation process. This improved method provides a greater amount of hydrophilic oxidized graphene material as compared to Hummers' method or Hummers' method with additional  $\text{KMnO}_4$ . The improved method is advantageous over the Hummers method. The protocol for running the reaction does not involve a large exothermic and produces no toxic gas. Moreover, the improved method yields a higher fraction of well-oxidized hydrophilic carbon material [51].



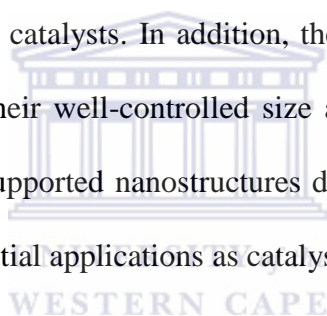
## 2.5 Platinum group metal nanoparticles

Platinum group metal nanoparticles are very much in demand and are vital for modern technology due to their outstanding catalytic properties. They have attracted much attention due to their unique performance in electronic, magnetic, optical and catalytic applications and many other fields [52]. Their application includes catalytic converters for catalytic control of car exhaust emissions, jewellery and watch making, chemical and petroleum refining industry (superb catalysts), electronics (hard drives), fuel cells (also as catalysts), liquid crystal display (LCD) glass and other glasses, anticancer drugs, spark plugs, electrodes, sensors, turbine engine coatings, medical components, dental alloys, etc. [53]. The use of platinum group metals as catalysts entails having major possible active surface which can deliver a maximum possible number of catalytically active sites. When using particles at the nanometer range, a high surface area to volume ratio is obtained as a catalytically active substance. The catalyst is either suspended in a reaction solution (quasi-homogeneous catalysis) or deposited on a particular support (heterogeneous catalysis). Dispersed and supported platinum group metal nanoparticles are used in the catalysis of a broad range of reactions: fuel-cell reactions, electron transfer reactions, hydrogenations, oxidations, decomposition reactions, etc. [53]

Platinum group metal nanoparticles can be prepared using various synthesizing techniques such as chemical reduction in a solution using hydrogen gas, alcohols, ethylene glycol, various hydrides or other reducing agents. These nanoparticles can also be prepared by electrochemical reduction, laser ablation of a platinum metal plate, micro-emulsion method, aerosol assisted deposition method or partial dissolution of Au-Pt nanoalloys [53, 54].

Platinum nanoparticles are usually found in the form of a suspension or colloid of submicrometre-size particles of platinum in a fluid, usually water. Pt nanoparticles have been subjected to intensive research for the design of electrodes. It is an essential catalyst for many chemical and electrochemical reactions, including oxygen reduction, hydrogen oxidation,

methanol oxidation and hydrogenations. Well-dispersed, small-sized Pt nanoparticles are expected to exhibit enhanced activity and selectivity for catalytic reactions [52]. Pd nanoparticles are of great importance as catalytic materials, as well as for a number of other applications such as hydrogen storage and sensing. The catalytic activity of these nanoparticles depends on their size and shape, and it has been shown that Pd nanoparticles of very sharp shapes exhibit strong catalytic activity for the organic reactions of Suzuki, Heck and Stille couplings [55]. They have reserved their catalytic properties in an aqueous suspension, which makes them the main study for the size dependence of the catalytic behavior. Presently, studies have been made for the issues of controlling the size and shape of Pd nanoparticles by the polyol method. They have been studied in the synthetic procedures for their potential applications as catalysts. In addition, the polyol method has been used to fabricate Pt nanoparticles with their well-controlled size and shape. Moreover, it has been shown that single, bimetal and supported nanostructures directly related to Pd nanoparticles have been exploited in their potential applications as catalysts [55, 56].



Platinum group metal nanoparticles can be prepared by the hydrothermal synthesis of platinum and the synthesis is based on the addition of tetramethylammonium hydroxide (TMAH) to the aqueous  $\text{PtCl}_4$ ,  $\text{IrCl}_3$  or  $\text{Rh}(\text{NO}_3)_3$  solution followed by the hydrothermal treatment of these precipitation systems at  $160^\circ\text{C}$  [53]. Polyvinylpyrrolidone (PVP) stabilized Pd nanoparticles of various shapes with the largest sizes in the forms of octahedrons (24 nm), tetrahedrons (22 nm) and cubes (20 nm) have been obtained by alcohol reduction in ethanol with the addition of a hydrochloric acid catalyst. Moreover, PVP–Pd nanoparticles of well-controlled spherical shapes have also been prepared by a modified polyol method. PVP–Pd nanoparticles of cubic, octahedral, tetrahedral and spherical shapes with well-controlled size achieved by using ethylene glycol (EG) as reductant and various inorganic species have also been fabricated [55, 56]. Au, Pt, Pd, Ru and Ir nanoparticles with a narrow size distribution

have been synthesized by chemical reduction of their corresponding metal species in ethylene glycol. In all cases, the average particle size was found to be smaller than 10 nm. Particle size was mainly controlled by varying the initial total metal concentration, the reaction temperature, and the concentration of PVP [57]. Therefore, platinum group metal nanoparticles are synthesized by the hydrothermal process, the polyol method and the chemical reduction of their corresponding metal species in ethylene glycol.



## Chapter 3

---

### EXPERIMENTAL METHODS

#### 3.1 Summary

This chapter describes the methods and procedures employed to synthesize the materials required in this work. It gives the synthesis methods used for graphene oxide, functionalized graphene oxide, platinum nanoparticles, platinum nanoparticles and platinum-palladium nanoalloy. It also includes the one step reduction of platinum, palladium and platinum-palladium nanoalloy being loaded onto the surface of the functionalized graphene oxide. Included here are the characterization techniques of the materials: spectroscopic (UV and FTIR), microscopic (HRSEM, HRTEM and XRD) and electrochemical (CV).

#### 3.2 Reagents

Graphite powder 1-2 micron, ACS reagents: potassium permanganate 99%, absolute ethanol ( $\geq 99,8\%$ ), aniline reagent ( $\geq 99,5\%$ ), ethylene glycol anhydrous (99,8%), palladium (II) chloride anhydrous 60% Pd basis, 2-propanol anhydrous (99,5%), ACS reagent chloroplatinic acid hexa-hydrate ( $\geq 37,50\%$ ) Pt basis, polyvinylpyrrolidone (PVP) average mol wt 40 000, hydrochloric acid ( $\geq 99,5\%$ ), sulphuric acid ( $\geq 99,8\%$ ), carbon black, lithium sulphate and lithium manganese oxide purchased from Sigma Aldrich. Hydrogen peroxide solution ultra ( $\geq 30\%$ ) RT trace analysis was purchased from Fluka.

#### 3.3 Instrumentation

All electrochemical measurements were done using Epsilon: Basi Electrochemistry Cell Stand integrated automated electrochemical work station from Bio Analytical Systems (BAS), Lafayette, USA. The Epsilon is generally used to study the electrochemical properties

of transition metal complexes or biosensors by the use of cyclic voltammetry, potential electrolysis and amperometry. All cyclic voltammograms were recorded with a computer interfaced with Epsilon: Basi Electrochemistry Cell Stand using an electrochemical cell 10 mL and three electrodes system. The electrodes which were used were; (1) glassy carbon electrode ( $0.071\text{cm}^2$ ) which acted as the working electrode, (2) platinum wire from Sigma Aldrich which acted as counter electrode and (3) Ag/AgCl from BAS kept in 3M NaCl acted as the reference electrode. Alumina micro polishing pads were obtained from Buehler, LL, USA and were used for polishing the glassy carbon electrode before modification.

Ultraviolet-visible (Uv-Vis) measurements were made using a Nicolet Evolution 100 UV-Visible spectrometer (Thermo Electron, UK) where the samples were placed in quartz cuvettes before analyses. The Nicolet is generally used to study absorption spectroscopy or reflectance spectroscopy in the ultraviolet-visible spectral region i.e. the UV-visible spectroscopy.

SEM images were taken with a Hitachi S3000N scanning electron microscope at an acceleration voltage of 20 kV at various magnifications. Small amounts of the materials (in powder form) were placed on copper grids. An aliquot of 2  $\mu\text{L}$  of each sample were drop coated on the copper grids and dried for two days at room temperature. The samples on the grids were coated with gold using a SC7640 Auto/ Manual high resolution super coater (Quorum Technology Ltd., England) at a voltage of 2 kV and plasma current of 25 mA for one minute.

HRTEM images were taken using Tecnai G2 F20X-Twin MAT 200kV Field Emission Transmission Microscopy from FEI (Eindhoven, Netherlands).

All FTIR spectra were recorded on spectrum 100 FTIR spectrometer (Perkin Elmer, USA) in a region of 400 to  $4000\text{ cm}^{-1}$ .

X-ray Diffraction using Diffractometer D8 Advance manufactured by Bruker AXS in Germany was done to determine the crystal structure identification of the samples. The instrument uses Cu-K-Alpha radiation (1.5406 angstroms) and Lynex Eye detector. It measures tube voltage of 40 kV, tube current of 40 mA and the variable slits are V20 variable slits.

### **3.4 Spectroscopic techniques**

#### **3.4.1 Fourier Transforms Infrared Spectroscopy**

Fourier transforms infrared spectroscopy is a powerful tool that determines the functional groups of materials and (IR) portion of the spectrum gives information that regards vibrational and rotational motion of atoms in molecules and is widely used for qualitative analysis. This technique is known to excite molecules to higher energy by absorbance of infrared radiation and the energy of absorbed IR radiation increases with amplitude of the vibrational motion of bonds in molecules [58]. In this study FTIR has been used to investigate the presence of the amine groups on graphene oxide once the graphene oxide was functionalized with aniline. The bonding interactions before and after graphene oxide was functionalized with aniline were investigated. The study by (Grinou et al) showed that the N-H and C-N group were found at 3000 and 3958  $\text{cm}^{-1}$  respectively. Similar results have been found in this study which confirms that there is a presence of amine groups on the functionalized graphene oxide.

### 3.4.2 UV-visible spectroscopy

Ultraviolet-visible spectroscopy (UV-vis) is a technique used for the determination of different analytes quantitatively. These include highly conjugated organic compounds, transition metal ions and biological molecules with respect to their electronic and optical properties. The most fundamental characteristic of absorption spectroscopy is the absorption of a discrete amount of energy. The energy of a photon absorbed or emitted during a transition from one molecular energy level to another is given by the equation:

$$E = h\nu \quad (3)$$

Where  $h$  is known as Planck's constant and  $\nu$  is the frequency of the photon. It is known that

$$c = \nu\lambda.$$

Therefore,

$$E = \frac{hc}{\lambda} \quad (4)$$

Therefore, the shorter the wavelength the greater the energy of the photon and the longer the wavelength, the lesser the energy of the photon. A molecule of any substance has an internal energy which can be considered as the sum of the energy of its electrons, the energy of vibration between its constituent atoms and the energy associated with rotation of the molecule. In a study of electronic properties of graphene oxide and functionalized graphene oxide, peaks appeared at 236 and a shoulder peak appeared at 244 nm for graphene oxide and at 222 and 271 respectively for functionalized graphene oxide. Their band gaps were calculated.



### **3.5 Microscopic techniques**

#### **3.5.1 High resolution scanning microscopy**

High resolution scanning electron microscopy (HRSEM) is one of the most powerful and important techniques that are used to study the surface morphology of a material. This technique has been designed in such a way that it can observe the fine details and fine structure of the surface of a material through the introduction of an electron beam deceleration method. A HRSEM image is known to tell the roughness, shape, particle size and porosity of a material. The surface of the graphene and functionalized graphene were observed to be not so rough but changed when the nanoparticles were loaded onto the surface and became very rough. The particle size was also obtained to be between 13.44 and 14 nm.

#### **3.5.2 High resolution transmission electron microscopy**

High resolution transmission electron microscopy (HRTEM) is a technique used to study the internal structure of a material. Not only is it used to study the internal structure but it is also used to study various characteristics of a material. It is used to study the shape, orientation, particle size, size distribution and lattice parameters of a material. HRTEM provides a direct link in the internal structure and its irregularities at the atomic scale and offers resolution to the Angstrom level and enables information to be obtained on the atomic packing rather than just the morphology of the sample. The technique uses phase contrast resulting from an interference of several beams and determines whether the particle that makes the specimen are dispersed or agglomerated. The technique is limited in high magnification imaging which requires high electron dose where by the specimen needs to be relatively insensitive. For graphene oxide independent nanosheets are observed and these should be wider in thickness and should be flat. In this study HRTEM was used to confirm the size and shape, distribution



and morphology of synthesized materials i.e. graphene oxide, functionalized graphene oxide and the functionalized graphene oxide-platinum group metal nanocomposites.

### **3.5.3 Energy dispersive spectroscopy**

This is an analysis technique usually used in conjunction with SEM and TEM. Energy dispersive spectroscopy (EDS) makes use of the X-ray spectrum emitted by a solid sample bombarded with a focused beam of electrons to obtain a localized chemical analysis. An electron beam typically 10-20 keV, strikes the surface of the conducting material causing X-rays to be emitted. Their energies depend on the material under examination. An image of each element in the sample can be obtained by scanning the electron beam across the material. It's a high-resolution variant of electron microprobe analysis/X-ray microanalysis whereby information can be obtained on the chemical composition of individual nanoparticles [60]. In this study EDS was used to obtain the elemental composition of the investigated samples.

### **3.6 X-ray diffraction**

X-ray diffraction (XRD) is a crystallinity technique for studying the crystal structure of a material and it is the only method that permits the direct identification of any crystalline material based on their unique crystal structure. Materials include minerals, metals, alloys, semiconductors, polycrystalline materials, superconductors, polymers, textile fibers, gemstones, proteins, as well as any other synthetic inorganic and organic crystals. XRD can also measure qualitative and quantitative phase analysis. The metal surface area of the materials used in this study could be determined using particle sizes obtained via XRD.

Crystalline structures have been found to have profound impacts on the electrochemical performance of the different materials. XRD was solely used to determine the crystal structure and particle size of the electrode materials. The Scherrer equation (eq 5) was used to determine the average particle size of the materials.

$$D = \frac{0.9\lambda}{\beta \cos\theta} \quad (5)$$

Where  $D$  is the mean size of the crystals, 0.9 is the shape factor,  $\lambda$  is the x-ray wavelength,  $\beta$  is the line broadening at half maximum intensity in radians and  $\theta$  is the Bragg's angle.

### 3.7 Electrochemical techniques

#### 3.7.1 Galvanostatic charge/discharge technique

This technique is a standard technique used to test the performance and cycle life of capacitors and batteries. A cycle is formed when there is a repetitive loop of charge and discharge. Normally, charge and discharge are conducted at constant current until a set voltage is reached. The charge (capacity) of each cycle is measured and the capacitance. Both are plotted as a function of cycle number. This curve is called the capacity curve. In practice, charge is commonly called capacity. Usually, capacity has the unit of ampere-hour (Ah) where 1 Ah = 3600 coulombs.

Since long cycle life is important to supercapacitors, the charge/discharge technique was employed to examine the service life of the electrode nanomaterials prepared in this study at a current density of 50 mA/g for 100 cycles. Eight electrode discs each with a diameter of 10 mm consisting of different material composites prepared was assembled in a double layer cell as a cathode and an anode in a symmetric cell. The Ag/AgCl reference electrode was used

and the separator was employed to stop the opposing electrodes from causing short circuit by touching one another. The cell was assembled in a small electrochemical button cell which consists of a stainless steel current collector with the same diameter as the working electrodes. The lithium manganese oxide (LMO) was used as the counter electrode. The two electrodes and the separator were soaked in the electrolyte solution first before being assembled in the electrochemical cell button. The electrolyte used was 1 M  $\text{Li}_2\text{SO}_4$ .

**Table 2: Parameters used for charge/discharge test**

Electrolyte	1 M $\text{Li}_2\text{SO}_4$
Current density	50 mA/g
Potential voltage window	Anode (0 to -0.9) V
	Cathode (0 to 0.9) V
Separator	Ag/AgCl reference electrode
Current collector	Stainless steel

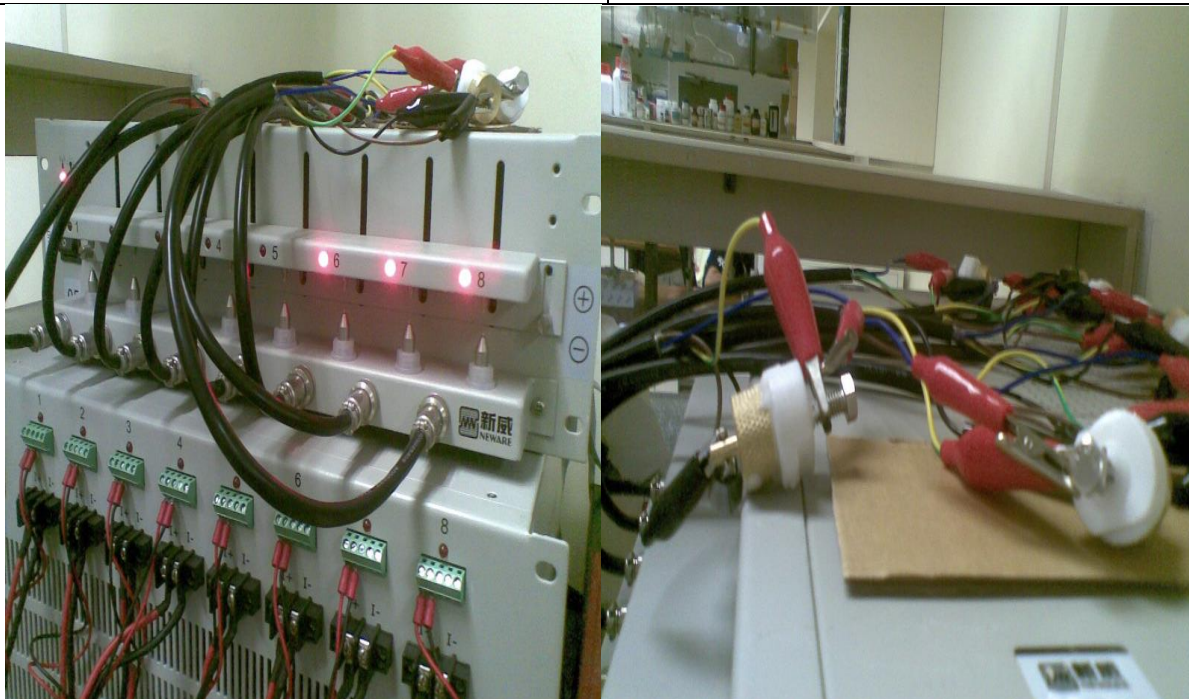


**Figure 7: The battery testing unit equipment connected to the monitor**

### **3.8 Experimental synthesis**

#### **3.8.1 Synthesis of graphene oxide using the Hummers method**

Graphene oxide was prepared by the simple Hummers method. Flake graphite was treated with potassium permanganate ( $\text{KMnO}_4$ ) and sulfuric acid ( $\text{H}_2\text{SO}_4$ ). Typical experimental method was as follow: 50 mL of  $\text{H}_2\text{SO}_4$  was added to a 250 ml flask filled with 2 g of flake graphite at room temperature and a black solution was formed. This was followed by the addition of 7 g of  $\text{KMnO}_4$  in an ice bath ( $0^\circ\text{C}$ ). A volume of 120 mL  $\text{H}_2\text{O}$  was added to the mixture followed by 30% wt of  $\text{H}_2\text{O}_2$  until there was no gas production. The solution was centrifuged and filtered. The brown powder formed (GO) was dried in a vacuum oven for 3 days [41, 61].



#### **3.8.2 Functionalization of graphene**

To functionalize the synthesized graphene oxide to prepare the aniline-functionalized graphene oxide, 0.2 g of GO was mixed with 4 g of aniline in 40 ml of deionized water and the solution was dispersed by sonication for 4 hours. The resulting solution was then washed with deionized water, filtered and dried at  $60^\circ\text{C}$  for 24 hours.

#### **3.8.3 Synthesis of PVP-palladium nanoparticles**

In a typical experiment, 0.6 g of  $\text{PdCl}_2$ , 6.0 mL of 0.2 M HCl and 300 mL of deionized water were mixed in a volumetric flask to form 2.0 mM  $\text{H}_2\text{PdCl}_4$ . The total volume was refluxed for 3 hours and was allowed to age for 2 days. The colour of the product was a typical pale-yellow colour. Then a volume of 15 mL of the 2.0 mM  $\text{H}_2\text{PdCl}_4$  solution was mixed with 25 mL of  $\text{H}_2\text{O}$ , 15 mL of ethanol and 0.6667g of PVP. They were refluxed for three hours under

air resulting in a dark brown solution. The solution was then filtered and dried at 60° C for 24 hours [61, 62].

### **3.8.4 Single step loading of metal nanoparticles on functionalized graphene oxide**

#### **3.8.4.1 Single step reduction of ionic platinum on functionalized graphene oxide**

Platinum nanoparticles were loaded on functionalized graphene oxide (f-GO) sheets by the chemical reduction of hexachloroplatinic acid ( $\text{H}_2\text{PtCl}_6$ ) in an ethylene glycol-water solution. Typically, 50 mg of f-GO was added in 50 ml of deionized water and sonicated for 15 minutes. A homogeneous solution was obtained. A 0.25 mg of aqueous solution of  $\text{H}_2\text{PtCl}_6$  was added to the above solution and sonicated for another 15 minutes. The mixture was added to 40 ml ethylene glycol in a 250 ml flask. The mixture was sonicated for 4 hours to ensure a uniform dispersion of  $\text{H}_2\text{PtCl}_6$  and f-GO in the ethylene glycol-water solution. The temperature was then elevated to 100°C and constantly stirred for 24 hours for reduction of graphene oxide to take place. The Platinum nanoparticles/functionalized graphene oxide composite was finally separated by filtration and washed several times with deionized water. The resulting product was dried under vacuum at 60°C for 24 hour [52].

#### **3.8.4.2 Single step reduction of palladium nanoparticles on functionalized graphene oxide**

Palladium nanoparticles were loaded on functionalized graphene oxide (f-GO) sheets by adding the synthesized palladium nanoparticles and treating with ethylene glycol-water solution. Typically, 50 mg of f-GO was added in 50 ml of deionized water and sonicated for 15 minutes. A homogeneous solution was obtained. 0.25 mg of palladium nanoparticles were added to the above solution and sonicated for another 15 minutes and the mixture was added to 40 ml ethylene glycol in a 250 ml flask. The mixture was sonicated for 4 hours to ensure a uniform dispersion of palladium nanoparticles and f-GO in the ethylene glycol-water

solution. The temperature was then elevated to 100°C and constantly stirred for 24 hours for reduction of graphene oxide to take place. The palladium nanoparticles/functionalized graphene oxide composite was finally separated by filtration and washed several times with deionized water. The resulting product was dried under vacuum at 60°C for 24 hour.

### **3.8.4.3 Single step reduction of palladium-platinum nanocomposites on functionalized graphene oxide**

Typically, 50 mg of f-GO was added to 50 ml of deionized water and sonicated for 15 minutes to obtain a homogeneous solution. A 0.25 mg of aqueous solution of  $\text{H}_2\text{PtCl}_6$  and 0.25 mg of palladium nanoparticles were added to the above solution and sonicated for another 15 minutes and the mixture added to 40 ml ethylene glycol in a 250 ml flask. The mixture was sonicated for 4 hours to ensure a uniform dispersion of  $\text{H}_2\text{PtCl}_6$ , palladium nanoparticles and f-GO in the ethylene glycol-water solution. The temperature was then elevated to 100°C and constantly stirred for 24 hours for reduction of graphene oxide to take place. The palladium nanoparticles-platinum nanoparticles-functionalized graphene oxide composite was finally separated by filtration and washed several times with deionized water. The resulting product was dried under vacuum at 60°C for 24 hour.

## **3.8.5 Fabrication of the electrode material**

### **3.8.5.1 Preparation of the electrode materials**

The materials used in the experiment for fabrication of the electrode consisted of 40 mg active material, 5 mg of carbon black, 5 mg (3 drops) of isopropanol and 8 mg of polytetrafluoroethylene (PTFE) binder. The active material consisted of the functionalized graphene oxide, the synthesized functionalized graphene oxide loaded with platinum

nanoparticles, functionalized graphene oxide loaded with palladium nanoparticles and finally the functionalized graphene oxide loaded with platinum-palladium nanocomposite. The carbon black and f-GO were mixed together and crushed to ensure that they were correctly mixed. For a given electrode, relevant materials were mixed together in a 10 mL small beaker to form dough. The dough was transferred onto a flat glass plate. A stainless steel/Teflon rod was used to roll the dough into mm thick flexible thin films. When making the thin film the dough was rolled many times with constant addition of three drops of isopropanol to ensure that the material was correctly mixed in the thin film. The thin film was then placed in an oven and was allowed to bake at 80° C under vacuum. Once the thin film was dry it was then cut into small wafers for the construction of the electrode.

#### **3.8.5.2 Construction of supercapacitor cell**

A single electrode was assembled with three parts; electrode material, stainless steel mesh current collector and stainless steel wire. The electrode was assembled by cutting the stainless steel mesh current collector into a 1 cm × 4 cm rectangular shape. The collector was then cleaned by shaking it in ethanol, drying it and then weighing. The approximately 1 cm<sup>2</sup> wafer was placed on the stainless steel mesh and pressed at a pressure of 20 MPa for 5 min. The electrode was then weighed and the difference in mass was used as the active mass of the electrode. The stainless steel wire was tightly held onto the current collector for external circuit connection. This fabrication acted as the cathode in the cell construction. The anode was made similarly, save for the active material. The active material for anode electrode was lithium manganese oxide (LMO). This method was used vice versa because it was not known yet if the materials used to make the thin films were a good anode material or good cathode material. The two were used to make a two-electrode asymmetric supercapacitor cell. The cell system was fabricated using 1 M Li<sub>2</sub>SO<sub>4</sub> solution as the electrolyte and tested for the

supercapacitor parameters using the BST8-3 eight-channel battery testing machine. The cell was made by holding together the two single electrodes (cathode and anode) with a porous and electronically non-conductive separator sandwiched between them to form the cell configuration.

### 3.9 Overview of main points

The characterization of the electrode materials was initiated by the investigation of the structural properties using quantitative and qualitative techniques such as, HRSEM, HRTEM, EDS, FTIR and XRD. Structural and electrochemical characterization and the techniques used for their study can be summarized as follows:

- The elemental composition of the functionalized graphene oxide/platinum group metal nanocomposites was quantitatively studied by the EDS
- The morphological properties and degree of agglomerations of the nanostructure were studied qualitatively by HRSEM.
- The crystallinity and the particle size of the electrode materials were qualitatively and quantitatively studied by XRD.
- Particle shape and distribution of the morphologies of the nanostructured graphene oxide and functionalized graphene oxide were qualitatively studied by TEM
- The stability and efficiency of the electrode material used in supercapacitors was tested by the galvanostatic charge-discharge test.
- The materials were tested for ethanol oxidation using CV.



## Chapter 4

---

### RESULTS AND DISCUSSION

#### 4.1 Summary

This chapter deals with presentation and discussion of experimental results. Results of characterization of materials using different techniques such as FTIR, UV, HRSEM, HRTEM etc are presented in this chapter.

#### 4.2 The Fourier Transform Infrared Spectrum of GO and f-GO

The FTIR was employed to investigate the bonding interactions in graphene oxide before the functionalization and after the functionalization with aniline. In the spectrum of GO (Fig.9), the peaks at 2858, 1624, 1387 and 1116  $\text{cm}^{-1}$  were assigned to the O-H stretching, C=O stretching, C-O stretching (carbonyl) and O-H bending vibrations respectively. Graphene oxide is a highly absorptive material as verified by its ability to become a gel like solution [23, 41]. The presence of these oxygen-containing groups reveals that the graphene has been oxidized. The polar groups, especially the surface hydroxyl groups, result in the formation of hydrogen bonds between graph

ene and water molecules; this further explains the hydrophilic nature of graphene oxide. The intensity of these peaks decreased significantly, and some of the peaks almost disappeared. When GO was chemically functionalized with aniline (f-GO), new peaks at 2958 and 1451  $\text{cm}^{-1}$  belonging to N-H and C-N stretching vibrations respectively appeared. The presence of these stretching vibrations confirm the presence of the amine groups of aniline on the GO surface which then confirms the successful functionalization of GO by aniline as a stabilizer [23]. Table 3, shows the peaks at their respectful frequencies.

**Table 3. Table showing the frequencies and the bonds found in graphene oxide and functionalized graphene oxide**

<i>Frequency <math>cm^{-1}</math></i>	<i>Bond</i>
2858	O-H stretching
1624	C=O stretching
1387	C-O stretching
1116	O-H bend
2958	N-H stretching
1451	C-N stretching

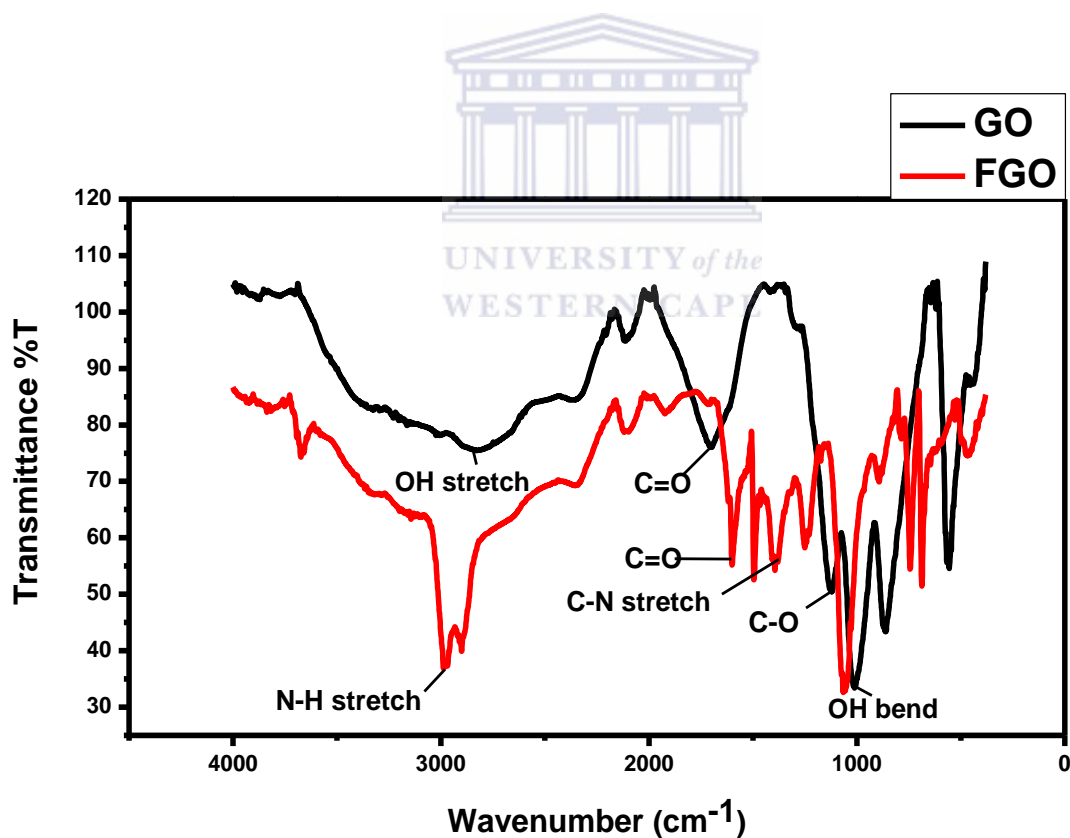


**Figure 8: FTIR spectrum of GO and f-GO**

### 4.3 UV-visible spectroscopy

From literature, the UV-vis absorption spectrum of graphene oxide (figure 9) shows maximum absorption peak at approximately 236 nm attributable to  $\pi$ - $\pi^*$  transition of the atomic C-C bonds and shoulder peak at approximately 304 nm due to  $\pi$ - $\pi^*$  transitions of aromatic C-C bonds [41].

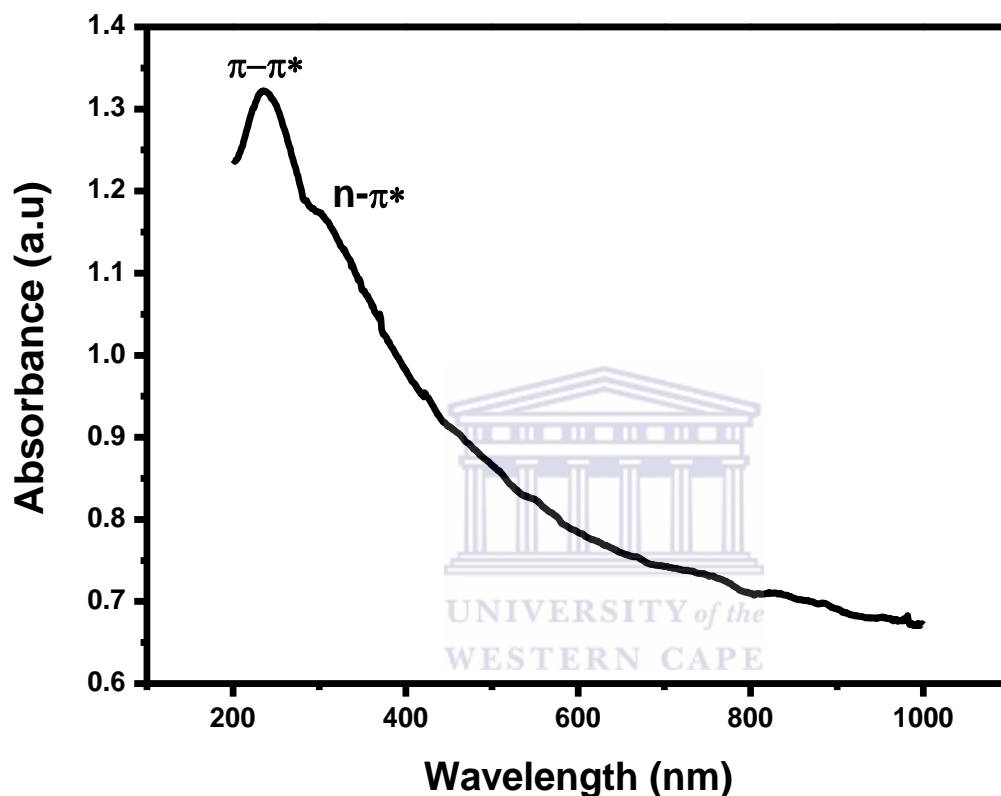


**Figure 9: UV-vis absorbance spectrum of GO**

Fig 10 shows the Uv-Vis spectra of graphene oxide and functionalized graphene oxide synthesized in this work. They were constructed to compare the optical properties of graphene oxide and those of the functionalized graphene oxide. The graphene oxide showed a peak at 236 nm which can be attributed to the  $\pi$ - $\pi^*$  transition of the atomic C-C bonds and a shoulder peak at approximately 304 nm due to  $\pi$ - $\pi^*$  transitions of aromatic C-C bonds. This compares very well with work of Shariyahry *et al* [41]. The functionalized graphene oxide

showed two bands at 222 and 271 nm with calculated band gaps of 5.35 eV and 4.58 eV respectively.

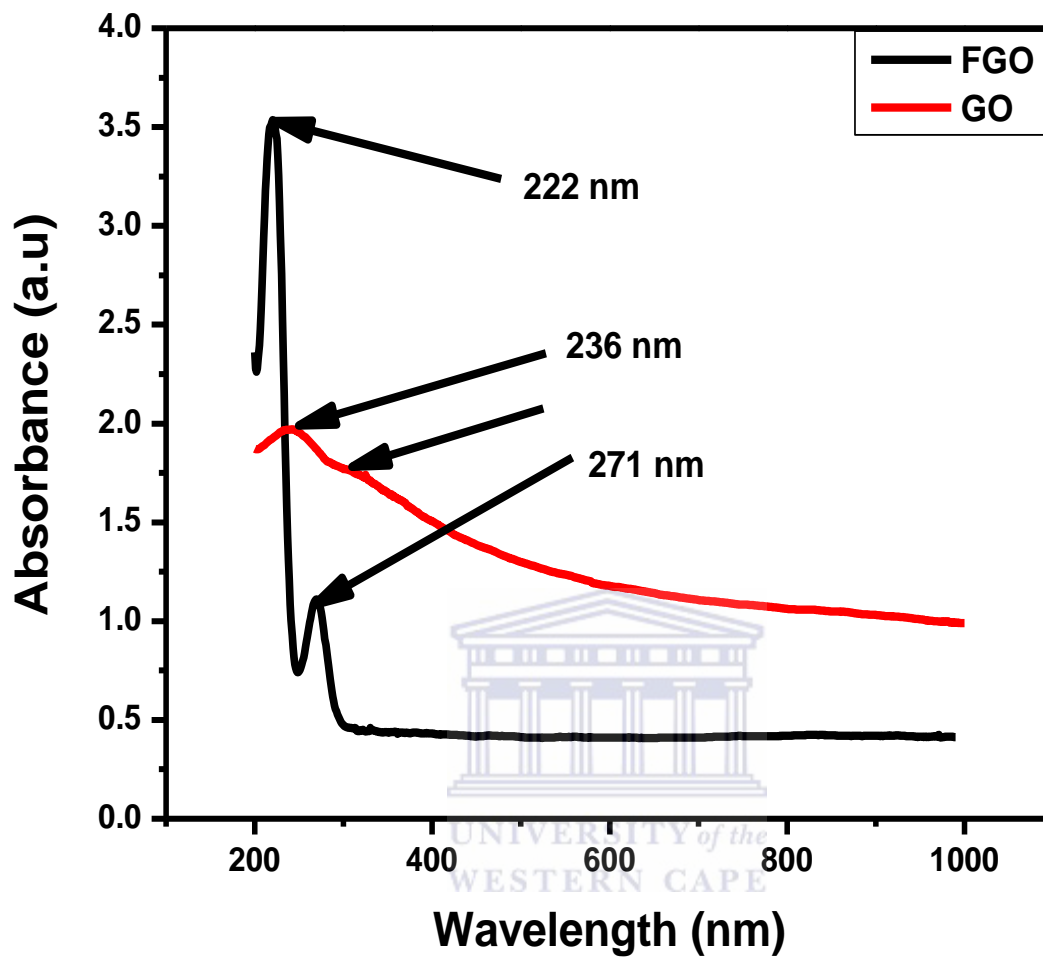
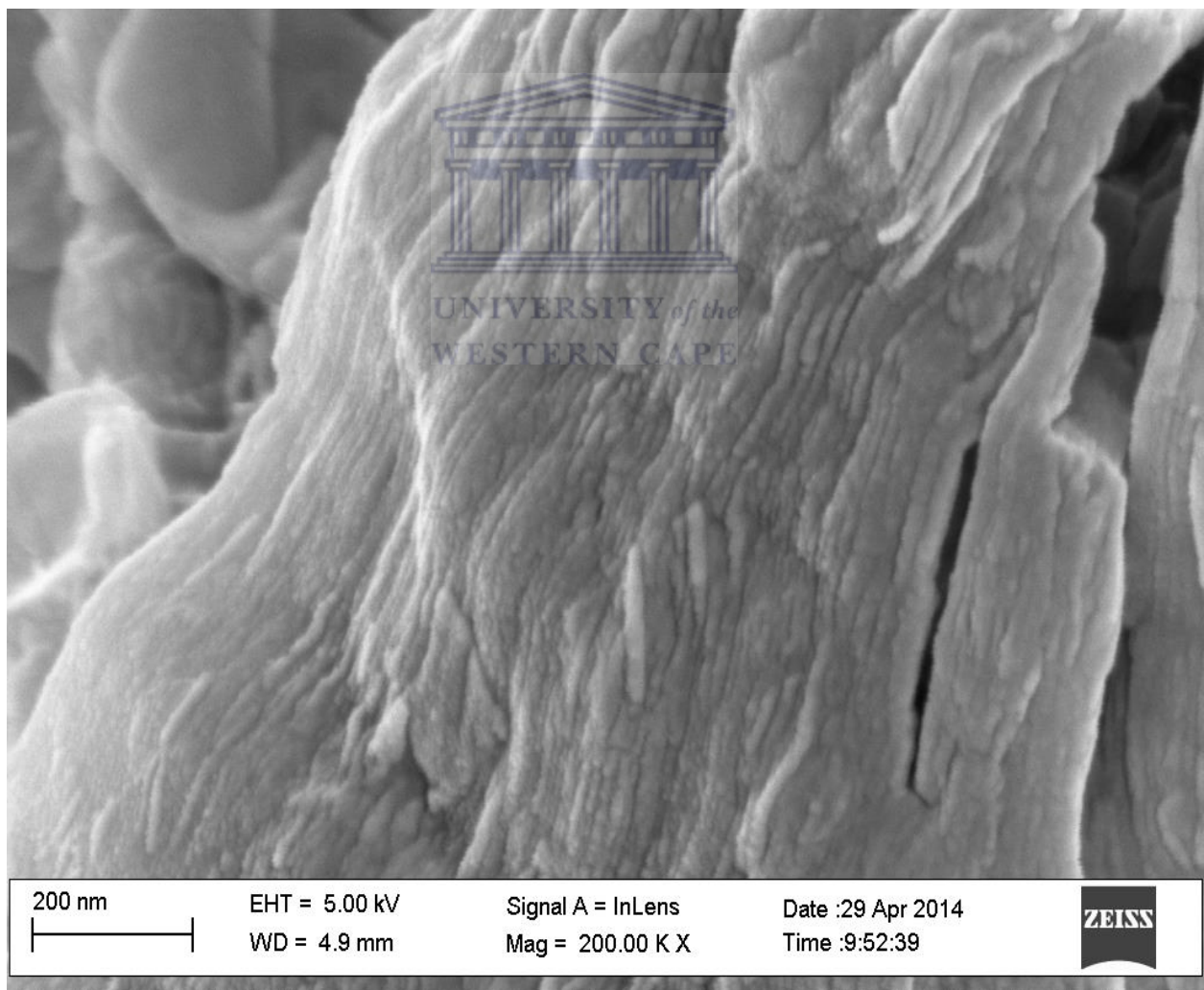


Figure 10: Uv-Vis spectra comparing the properties of GO and f-GO

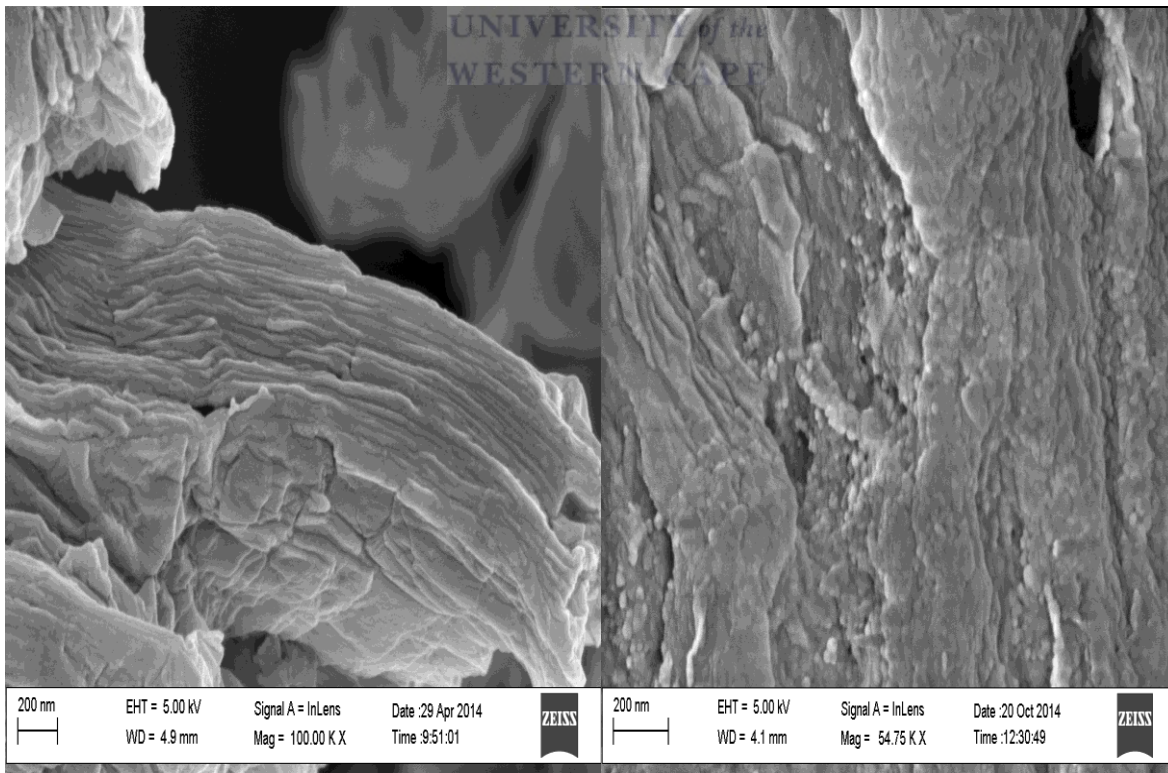
#### 4.4 High Resolution Scanning electron microscope

A scanning electron microscopy image reveals the internal structures of nanoparticles. The image formed is due to secondary electrons transmitted by the sample surface following excitation by the primary electron beam. From literature, the SEM image of graphene (figure 11), can be observed to have a layered structure of ultrathin and homogeneous graphene films [55]. Such films are folded or continuous at times and it is possible to distinguish the edges of individual sheets from the image, including kinked and wrinkled areas. It reveals a crumpled and rippled structure which might be due to the deformation upon the exfoliation and restacking process [41].



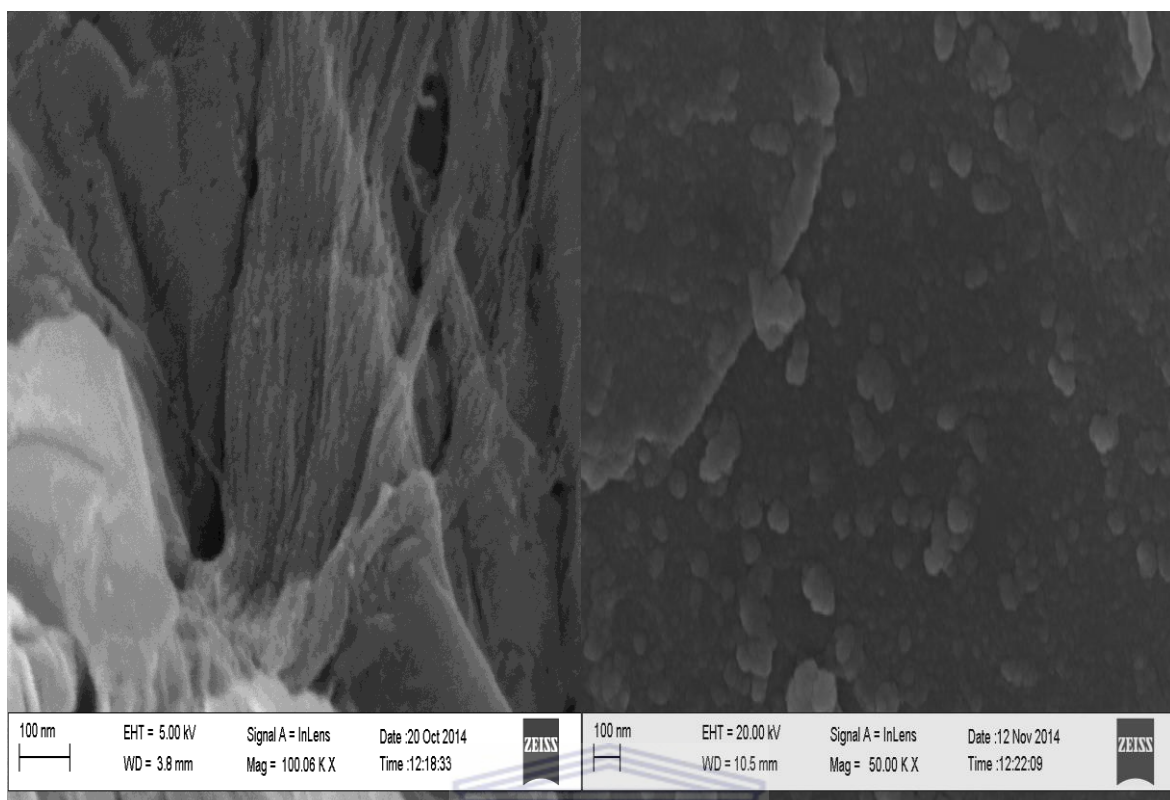
**Figure 11: SEM image of GO**

Figure 12 shows the SEM images of the different nanomaterials synthesised in this work. The SEM image of f-GO (figure 12a), shows a layered structure of ultra-thin and homogeneous graphene films. It also shows that the graphene films are entangled with each other. The SEM image of f-GO-Pd (figure 12b) shows that the palladium nanoparticles were successfully loaded onto the surface of graphene oxide. The surface became very rough with small particles evident on the surface. In figure 12c, the Pt particles are spread out on the graphene sheets and when magnified a uniform distribution of Pt nanoparticles can be observed. We can therefore conclude that the platinum nanoparticles were successfully loaded onto the surface of the functionalized graphene oxide. The SEM image of the nanocomposite f-GO-Pd-Pd shown in (figure 12d) shows a very rough surface with evidence of nano clusters. The aggregated clusters of Pt and Pd particles can be seen in a magnified view of the graphene sheet. Pt nanoparticle aggregation is an important concern in the development of electro-catalyst films since it can significantly decrease the surface area [52].



**a**

**b**



**c**

**d**



**Fig 12: SEM images of a. f-GO, b. f-GO-Pd, c. f-GO-Pt, d. f-GO-Pd-Pt**

#### 4.5 High Resolution Tunneling Electron Microscopy

Tunneling electron microscopy is known to provide information on particle size, shape & crystallography of nanoparticles. The TEM image of GO (figure 13a) retains a graphene-like lattice substructure [50]. It shows that the nanosheets are observed to be larger than 1.5 $\mu\text{m}$  in width and are flat. This is due to sonication when preparing the TEM samples. It destroys the Van der Waals interactions between GO layers. The large nanosheets were observed to be situated on top of the grid, resembling a wavy silk veil [51]. The sheets are transparent and entangled with one another. It also shows the existence of large amount of oxygen containing functional groups on the surface of GO sheets. The TEM image of f-GO (figure 13b) shows a lot of wrinkles with the particles being denser when the GO was modified with aniline, an indication of successful functionalization of GO with aniline.

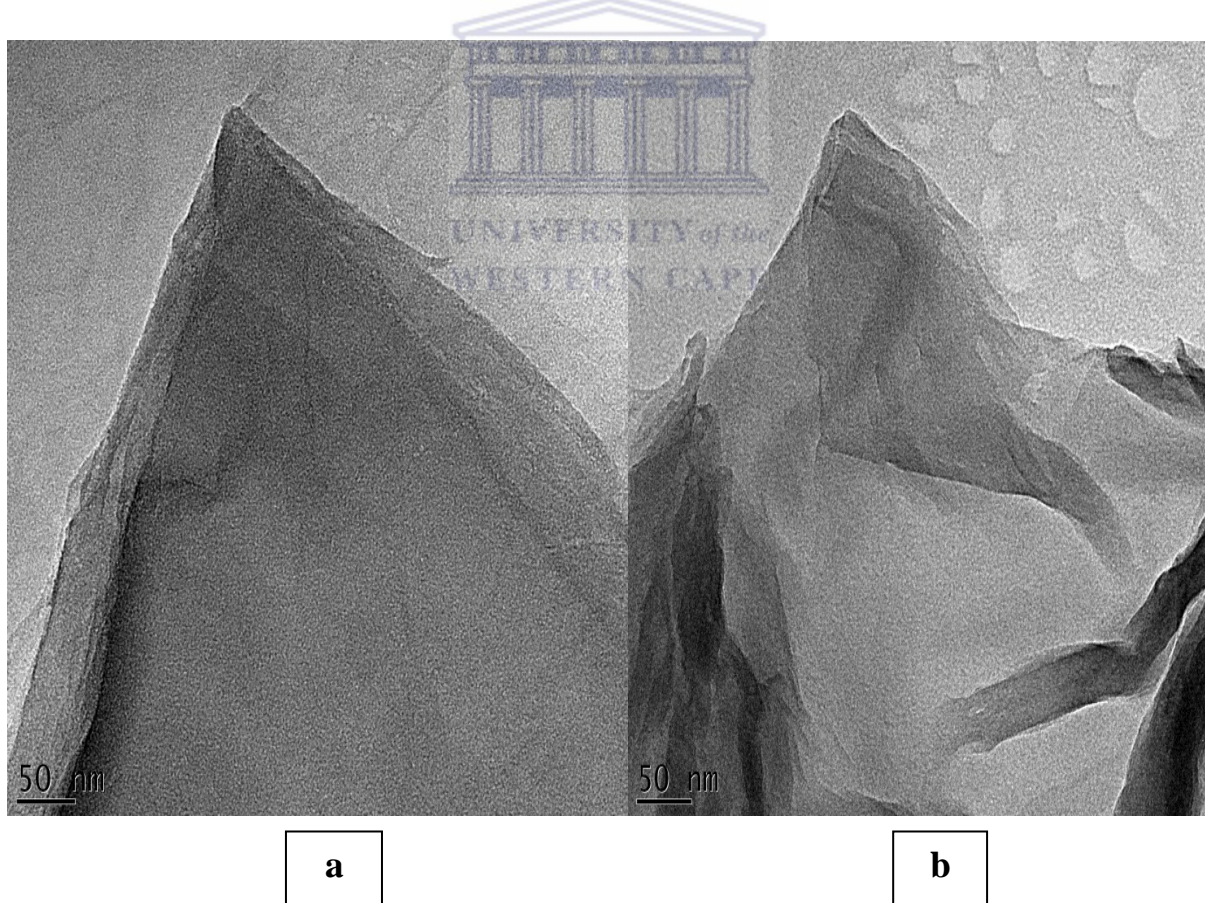
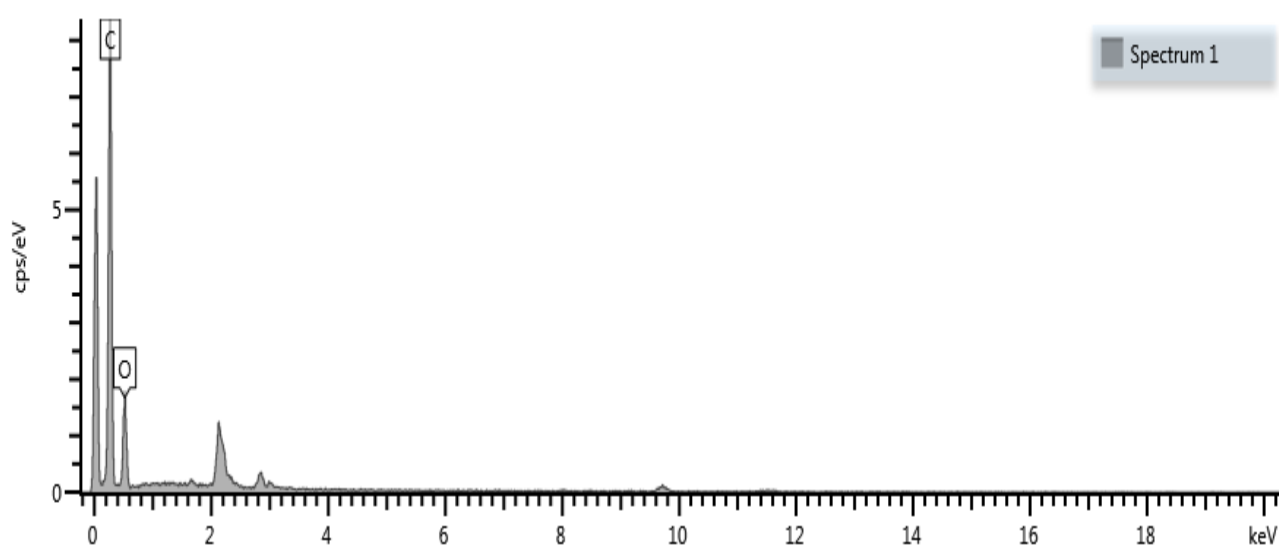


**Figure13. TEM images of; a. GO and b. f-GO**

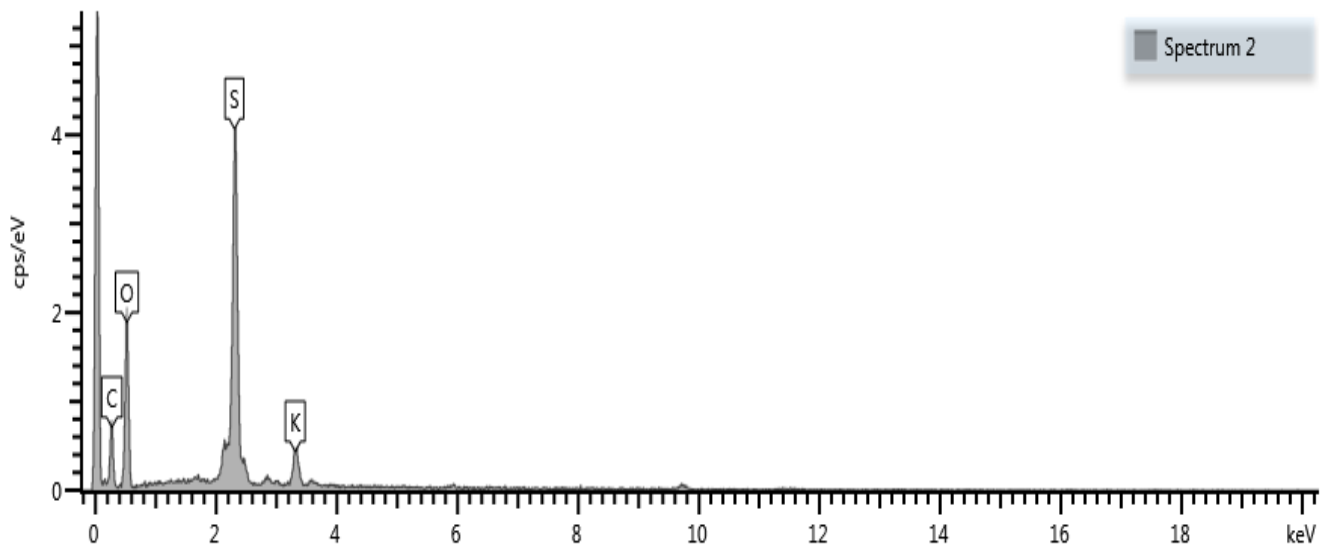


#### 4.6 Energy dispersive spectroscopy

The EDS analysis was used to study the elemental composition of the nanocomposite materials. Figure 14a shows the spectroscopy of the graphene oxide as synthesized by the simple Hummers method, the spectroscopy shows that the graphene oxide sample contained carbon (in abundance) and oxygen. This is as is expected of graphene oxide since graphene oxide contains various oxygen containing functional groups and these oxygen functional groups have been identified as mostly in the form of hydroxyl and epoxy groups with smaller amounts of carboxyl, carbonyl, phenol, lactone, and quinone at the sheet edge [35, 38]. Figure 14b shows that the functionalized graphene oxide contained some few traces of the sulphur (S) and potassium (K) elements which could be due to some contamination during the preparation of the SEM samples or inadequate washing of the oxidized graphene oxide. Figure 14c shows the elemental composition of the nanocomposite FGO-Pd-Pt. It shows that Pd and Pt are present in the sample even thou they do not appear in abundance and Cl can be due to impurities in the sample. This confirms that the loading of the nanoparticles on the surface of functionalized graphene oxide was successful.



a



**b**



**c**

**Figure 14: EDS spectroscopy of a. GO, b. f-GO and c. f-GO-Pd-Pt nanocomposite**

**Table 4: Elemental compositions study obtained with EDS**

Element	FGO (%)	GO (%)	FGO-Pd-Pt (%)
<b>C</b>	<b>50.51</b>	<b>74.57</b>	<b>31.96</b>
<b>O</b>	<b>39.83</b>	<b>25.43</b>	<b>66.5</b>
<b>Pd</b>	-	-	<b>0.13</b>
<b>Pt</b>	-	-	<b>1.22</b>
<b>K</b>	<b>1.22</b>	-	-
<b>S</b>	<b>8.44</b>	-	-
<b>Cl</b>		-	<b>0.19</b>



#### 4.7 X-ray diffraction (XRD)

Figure 15 shows the X-ray diffraction patterns of f-GO, f-GO-Pd, f-GO-Pt and f-GO-Pd-Pt. The peak at  $9.5^\circ$  was assigned to the characteristic diffraction peak (002) of reduced GO (by ethylene glycol), corresponding to the removal of a large number of oxygen-containing groups. This was attributed to the GO nanosheets being partially reduced to graphene and restacked into an ordered crystalline structure [23]. The diffraction peak at approximately  $43^\circ$  corresponds to the (100) plane of the hexagonal structure of GO meaning this plane is also present on the functionalized graphene oxide. For the f-GO-Pd, f-GO-Pt and f-GO-Pd-Pt nanocomposite the position of the (002) diffraction peak (at  $9.5^\circ$ ) moved slightly to a lower angle (at  $6^\circ$ ) after the deposition of the nanoparticles on the surface of the functionalized graphene oxide, which indicates that GO is further transformed to the crystalline graphene, and the conjugated graphene network ( $sp^2$  carbon) has been re-established by the reduction process. Platinum group metal nanoparticles are suggested to play an important role in the

reduction of GO when using ethylene glycol as a reducing agent [23, 26]. Further crystalline palladium showed peaks at 9.2°, 21° and 39° which were assigned to the (111), (200) and (220) planes respectively. For the crystalline platinum, diffraction peaks appeared at 8.2°, 18° and 42° which were assigned to (112), (210) and (310) crystalline planes of face-centered-cubic (fcc) Pt nanoparticles respectively, indicating a fcc structure. Lastly f-GO-Pd-Pt showed diffraction peaks at 18.4° and 43° which belong to crystalline platinum at planes (210) and (310) respectively. Crystalline palladium diffraction peaks 39° and 48° belong to (310) and (350) planes respectively [23].

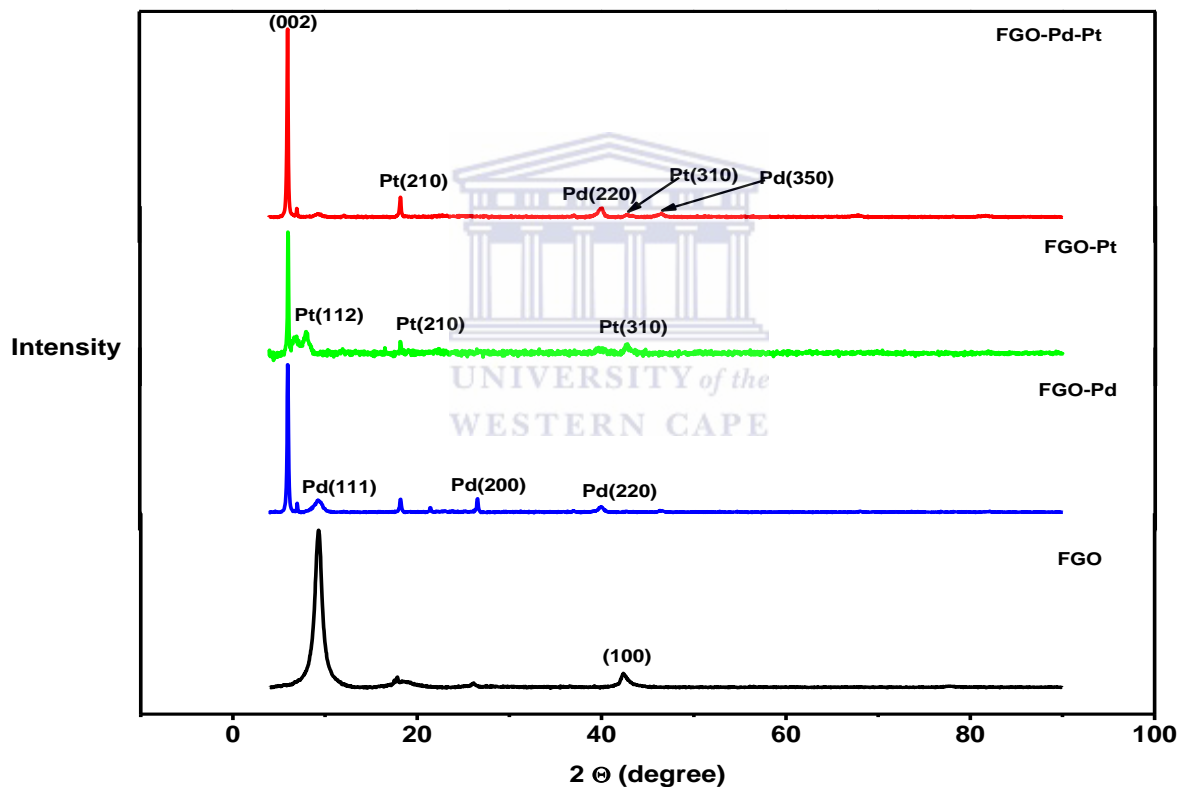


**Figure 15: X-ray powder diffraction (XRD) patterns of FGO, FGO-Pd, FGO-Pt and FGO-Pd-Pt**

#### 4.8 Galvanostatic charge/discharge test

The charge/discharge test is one of the most important techniques that are used to determine the specific capacitance of a supercapacitor. It is used to test for the performance, cycle life and the long term stability of energy storage devices such as batteries and supercapacitors.

##### 4.8.1 Testing carbon black as a supercapacitor material

Figure (16a) shows the cycle life of carbon black as an anode material. It was one of the materials used in the construction of the electrode materials. Carbon black is a good material to mix other materials with due to its impressive properties such as good electrical conductivity, particle size, structure and its surface chemistry. The cycle life of carbon black was tested in order to compare it with that of the functionalized graphene oxide. Mass of the thin film of carbon black was 4.608 mg and the first cycle charge and discharge capacities obtained were 0.83 mAh/g. Voltage/time cycling plot of carbon black was cycled in the anode (negative electrode). The voltage range was 0 to -0.9 V vs. Ag/AgCl. Cycling was done at a current density of 50 mA/g in 1 M Li<sub>2</sub>SO<sub>4</sub> (aq). The specific discharge capacity was found to be 0.97 mAh/g. The specific discharge capacitance is then calculated as follows:

$$\text{Specific discharge capacitance} = \frac{(0.97 \times 3.6)}{0.9} = 3.9 \text{ F/g} \quad [64, 65]$$

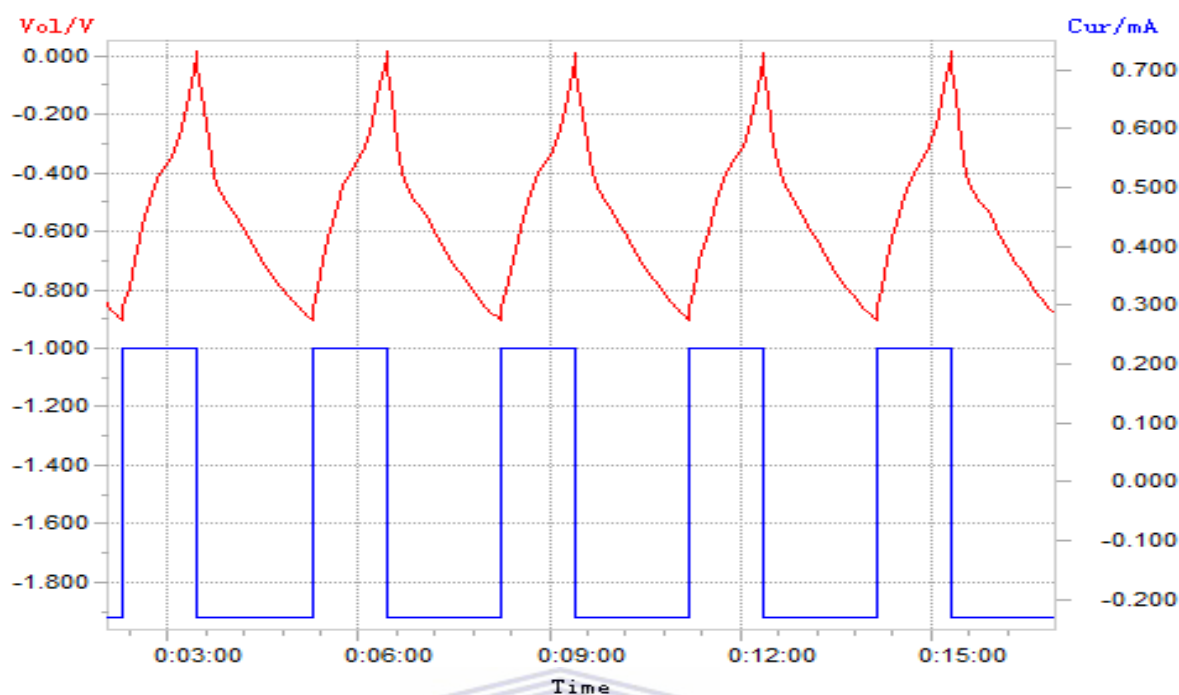


**Figure 16a. Cycling plot of carbon black cycled in the anode (negative electrode)**

Figure (16b) shows the cycle life of carbon black as a cathode material. Mass of the thin film of carbon black was 4.608 mg and the first cycle charge and discharge capacities obtained were 0.83 mAh/g. Voltage/time cycling plot of carbon black was cycled in the cathode (positive electrode). The voltage range was 0 to -0.9 V vs. Ag/AgCl. Cycling was done at a current density of 50 mA/g in 1 M Li<sub>2</sub>SO<sub>4</sub> (aq). The specific discharge capacity was found to be 0.6 mAh/g. The specific discharge capacitance is then calculated as follows:

$$\text{Specific charge capacitance} = \frac{(0.6 \times 3.6)}{0.9} = 2.4 \text{ F/g} \quad [64, 65]$$

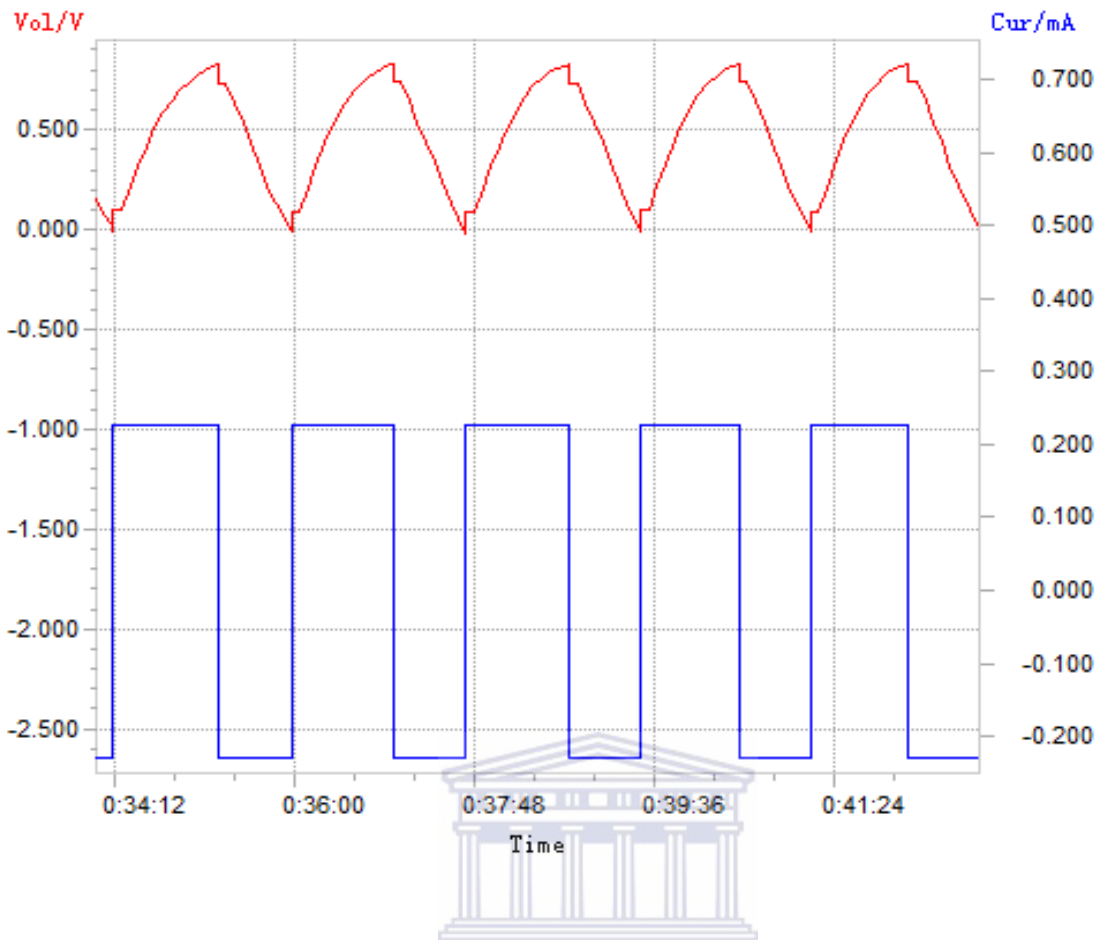


**Figure 16 b. Cycling plot of carbon black cycled in the cathode (positive electrode)**

From the values of the specific charge and discharge capacitance, we can observe that the specific discharge capacitance is greater as compared to the specific charge capacitance. This therefore means that carbon black is better as an anode material than as a cathode material. Beyond the given voltage range +0.9V carbon black reaches oxygen evolution.

#### 4.8.2 Testing functionalized graphene oxide as a supercapacitor material

Figure 17a shows the cycle life of functionalized graphene oxide as an anode material. Mass of the thin film for the electrode material was measured as 2.896 mg. The voltage range was 0 to -0.65V vs. Ag/AgCl) at a current density of 50 mA/g in 1 M Li<sub>2</sub>SO<sub>4</sub> (aq). Specific discharge capacity was found to be 3.3 mAh/g. The specific discharge capacitance is calculated as follows:

$$\text{Specific discharge capacitance} = \frac{(3.3 \times 3.6)}{0.65} = 18.27 \text{ F/g} \quad [64,$$

65]

However, hydrogen evolution occurred at -0.7V vs. Ag/AgCl, which therefore limited the lowest achievable voltage to (-0.65V vs. Ag/AgCl). This is a disadvantage as a greater value of specific discharge could have been obtained if hydrogen evolution couldn't have been a problem. The functionalized graphene oxide also showed high resistance and therefore it is not a good anode material.



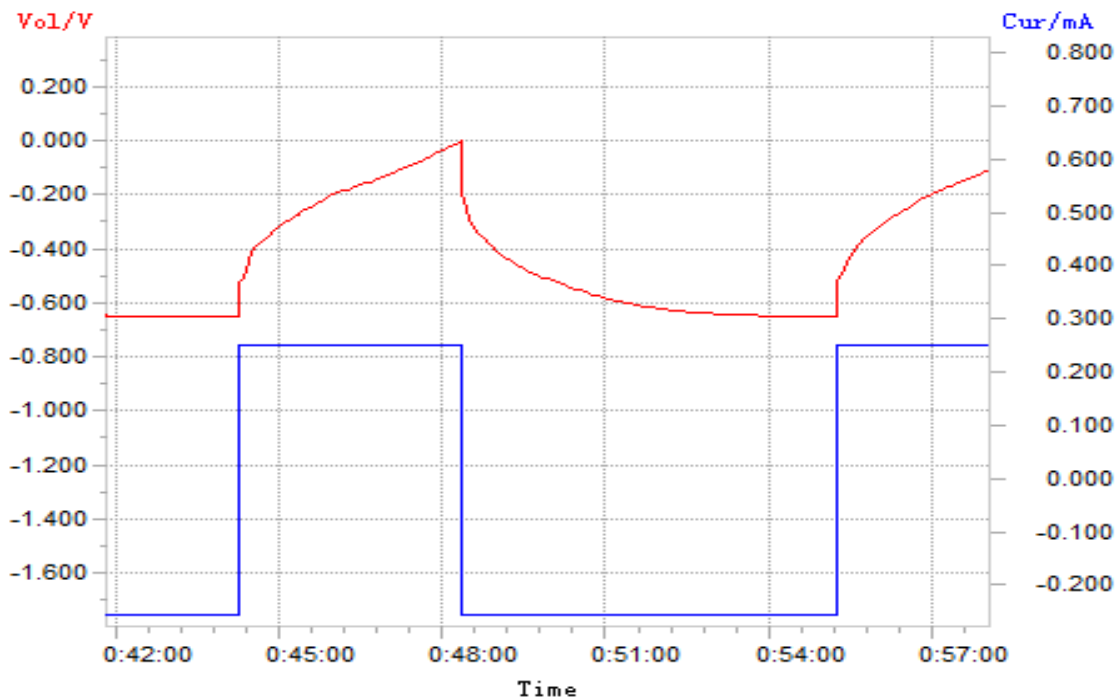


**Figure 17 a. Cycling plot of functionalized graphene oxide cycled in the anode (negative electrode)**

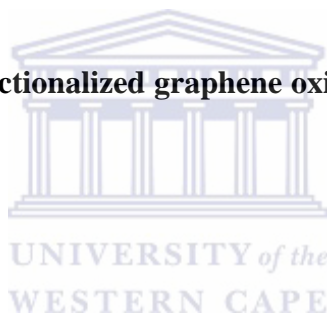


Figure (18 b) shows the cycle life of functionalized graphene oxide as a cathode material. Mass of the thin film for the electrode material was measured as 2.896 mg, voltage range was 0 to +8.5 V vs. Ag/AgCl at a current density of 50 mA/g in 1 M Li<sub>2</sub>SO<sub>4</sub> (aq). Specific charge capacity was found to be 0.35 mAh/g. Specific discharge capacitance was therefore calculated as follows:

$$\text{Specific charge capacitance} = \frac{(0.35 \times 3.6)}{0.85} = 1.5 \text{ F/g} \quad [64,$$

65]

**Table 5: Capacitance values of different materials**

<b>Material</b>	<b>Charge Capacity (mAh/g)</b>	<b>Charge Capacitance (F/g)</b>	<b>Discharge Capacity (mAh/g)</b>	<b>Discharge Capacitance (F/g)</b>
<b>Carbon black</b>	<b>0.6</b>	<b>2.4</b>	<b>0.97</b>	<b>3.9</b>
<b>f-GO</b>	<b>0.35</b>	<b>1.5</b>	<b>3.3</b>	<b>18.27</b>

However functionalized graphene oxide has high discharge resistance in the cathode voltage range evident by the more than 0.5V voltage drop between charge and discharge. This cathode voltage drop limits the functionalized graphene oxide from obtaining a greater value of specific charge capacitance. f-GO provided the highest specific capacity of 18.27 F/g as an anode in 1M Li<sub>2</sub>SO<sub>4</sub> (aq) electrolyte. High resistance on discharge as a cathode in the same electrolyte produced negligible specific capacitance in the cathodic range. The energy that goes into the system should approximately be the same as the energy that gets discharged out of the system. This is not the case with the cathode electrode. We can therefore say that functionalized graphene oxide is not a good anodic or cathodic material and therefore it cannot be used in applications as novel supercapacitor material.

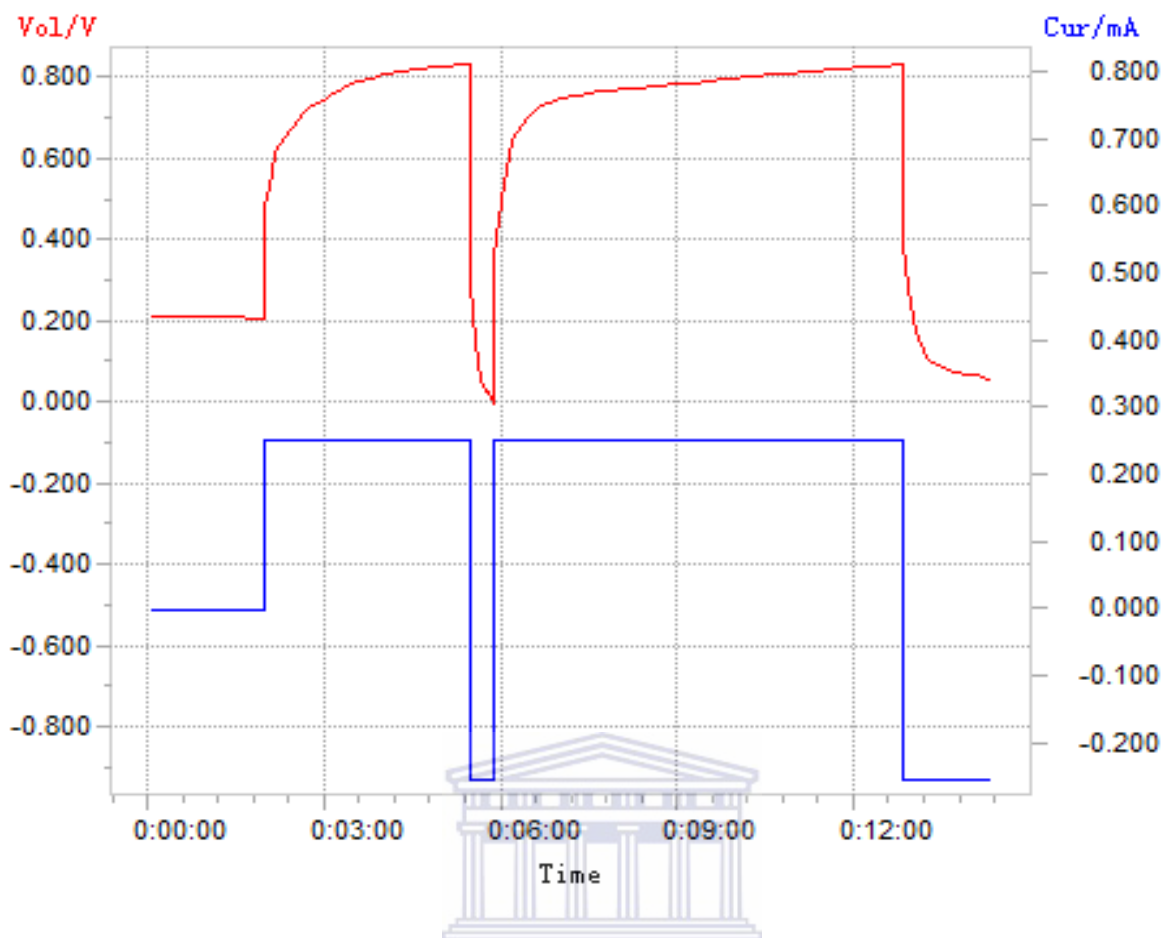
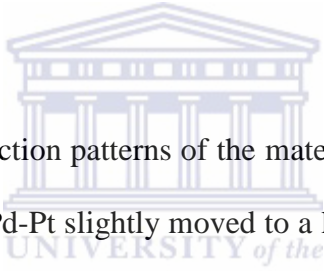


**Figure 17b. Cycling plot of functionalized graphene oxide cycled in the cathode (positive electrode)**

We can conclude from the results above that carbon black makes a good anodic material for supercapacitors while functionalized graphene oxide is not a good or ideal material for application in supercapacitors as it is neither a good anode nor a good cathode. There are possible reasons why the materials did not give the best results. These include problems in the preparation method of the functionalized graphene oxide. The aniline that was used to functionalize graphene oxide must have not been pure. Some impurities might have been introduced during the preparation of the nanomaterials, etc. Therefore, the Galvanostatic charge/discharge test was not conducted for the other materials as they all contain the functionalized graphene oxide. The functionalized graphene oxide rendered the other materials not ideal materials for application in supercapacitors.

### CONCLUSIONS AND RECOMMENDATIONS

In summary, graphene oxide was synthesized and functionalized with aniline. The aniline served as a stabilizer during the loading of the platinum group metal nanocomposites on the surface of the functionalized graphene oxide. The platinum group metal nanoparticles were successfully loaded onto the surface of the graphene oxide and this was proven by FTIR and EDS. The overall objective was to study the characteristics of the functionalized graphene oxide/platinum group metal nanocomposites electrode material by using both qualitative and quantitative tools.

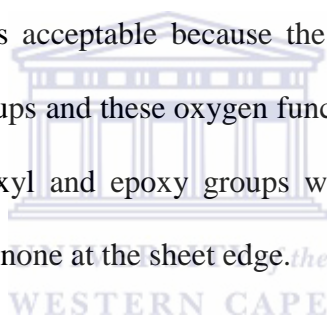


As observed from the XRD diffraction patterns of the materials, the diffraction peak (002) in the f-GO-Pd, f-GO-Pt and f-GO-Pd-Pt slightly moved to a lower angle after the deposition of the nanoparticles on the surface of the functionalized graphene oxide which indicates that GO is further transformed to the crystalline graphene and the conjugated graphene network ( $sp^2$  carbon) has been re-established by the reduction process. The XRD patterns of the materials showed peaks that were weak and poorly developed which could be the result of loss of water contents causing variation in crystal lattice.

The morphological features of the electrode materials were studied with the HRSEM and the HRTEM. The SEM showed roughness on the surface of the functionalized graphene oxide and further magnification showed uniform dispersion of the platinum and palladium nanoparticles on the surface of the functionalized graphene oxide. The aggregated clusters of Pt and Pd particles can also be seen in a magnified view of the graphene sheet.

HRTEM shows that the nanosheets are observed to be larger than 1.5 $\mu\text{m}$  in wideness and are flat which is due to sonication when preparing the samples for TEM analysis. This destroys the Van der Waals interactions between GO layers. The large nanosheets were observed to be situated on top of the grid, resembling a wavy silk veil. The sheets are transparent and entangled with one another. It also shows the existence of large amount of oxygen containing functional groups on the surface of GO sheets. The HRTEM image of f-GO showed a lot of wrinkles and the particles are denser when the GO was modified with aniline, showing that aniline was successfully functionalized with GO.

EDS showed the elemental composition of the GO, f-GO and f-GO-Pd-Pt with carbon and oxygen being in excess which is acceptable because the graphene oxide contains various oxygen containing functional groups and these oxygen functional groups have been identified as mostly in the form of hydroxyl and epoxy groups with smaller amounts of carboxyl, carbonyl, phenol, lactone, and quinone at the sheet edge.



FTIR showed strong peaks of oxygen-containing groups. Their presence reveals that graphite has been oxidized. The polar groups, especially the surface hydroxyl groups, result in the formation of hydrogen bonds between graphite and water molecules; this further explains the hydrophilic. It also showed the strong peaks of N-H and C-N which belong to the aniline and this confirms that aniline did indeed functionalize the graphene oxide.

Uv-Vis absorption spectra showed that graphene oxide showed a peak at 236 nm which is attributed to the  $\pi\text{-}\pi^*$  transition of the atomic C-C bonds and a shoulder peak at approximately 304 nm due to  $n\text{-}\pi^*$  transitions of the aromatic C-C bonds. The functionalized graphene oxide showed two bands at 222 and 271 nm with calculated band gaps of 5.35 eV

and 4.58 eV respectively. The test of the materials by galvanostatic charge-discharge proved the nanomaterials are not good for applications as supercapacitor electrode material. We can conclude from the results that carbon black makes a good anodic material for supercapacitors while functionalized graphene oxide is not a good or ideal material for application in supercapacitors as it is neither a good anode nor cathode. f-GO provided the highest specific capacitance of 18.27 F/g as an anode in 1M Li<sub>2</sub>SO<sub>4</sub> (aq) electrolyte. High resistance on discharge as a cathode in the same electrolyte produced negligible specific capacitance in the cathodic range. The energy that was put into the system was not the same or even close to the energy that got out of the system. We can therefore conclude that the prepared materials are not good materials for application in supercapacitors and they are not good catalysts as well.

## 5.1 Future works and recommendations

Recommended future work would include;

- Employ the quantitative technique like thermogravimetric analysis (TGA) in order to find the amount of water present and also observe structural transformation of the f-GO
- Ideally, the slower scan rate (1mV/s to 5mV/s) is more feasible in order to achieve the ideal capacitive behaviour
- Compare different electrolytes like NaCl, Li<sub>2</sub>SO<sub>4</sub>, KCl, HNO<sub>3</sub>, etc., since a material behaves differently to every cation or anion.
- The main recommendation from this study is to employ other materials like highly activated carbon (e.g CNTs, graphite etc.) and conducting polymers (e.g PANI, PEDOT etc.) as anodes and the materials as cathode when assembling the cells. These hybrid systems should exhibit superior capacitive behaviour in comparison.

## REFERENCES

1. Compton O. C, Nguyen S. T, (2010). "*Graphene oxide, highly reduced graphene oxide, and graphene: versatile building blocks for carbon-based materials,*" *Small*, 6(6), 711– 723
2. Hsia-San Shu F. (2011). "*Global change and energy crisis*". *Energy*, 23, 119-199
3. Mediavilla M, Miguel L. J., Castro C. (2010). "*From fossil fuels to renewable energies*". *Energy*, 16, 56-193
4. Burke A. (2000). "*Ultracapacitors: why, how, and where is the technology.*" *Journal of Power Sources*, 91(1), 37-50
5. Conway B. E. (1999). "*Electrochemical Supercapacitors: Scientific Fundamentals and Technological Applications*". New York, Kluwer-Plenum, 125(3), 809-912
6. Chu A. P., Braatz P (2002). "*Comparison of commercial supercapacitors and high-power lithium-ion batteries for power-assist applications in hybrid electric vehicles I. Initial characterization.*" *Journal of Power Sources*, 112(1), 236-246
7. Marin S. Halper, James C. Ellenbogen. (2006). "*Supercapacitors: a brief overview.*" *Mitre-nanosystems group*, 17, 632-785
8. Illinois Capacitor Inc, [www.illcap.com](http://www.illcap.com)
9. Ferrando R, Jellinek J, Johnston R. L, (2008). "*Nanoalloys: From Theory to Application of Alloy Clusters and Nanoparticles*", *Chemical Reviews*, 108(3), 846-904
10. Zhu Y , Murali S, Cai W, Li X, Suk J. W, Potts J. R, Ruoff R. S. (2010). "*Graphene and Graphene Oxide: Synthesis, Properties, and Applications*". *Advanced Materials*. 2010, (20), 1–19

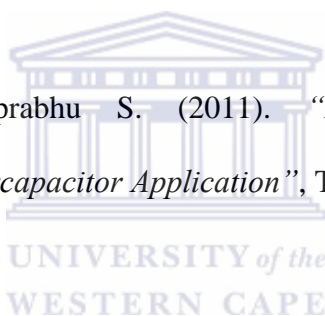
11. Dreyer D. R, Park S, Bielawski C, Ruoff R. S. (2007). "*The chemistry of graphene oxide*". Chemical Society Reviews, 56(11), 899-1045
12. Grinou A, Yun Y.S, Cho S. Y, Park H. Y, Jin H-J. (2012). "*Dispersion of Pt Nanoparticle-Doped Reduced Graphene Oxide Using Aniline as a Stabilizer*". Materials 5, 2927-2936
13. Li Y, Gao W, Ci L, Wang C, Ajayan P. M. (2011). "*Catalytic performance of Pt nanoparticles on reduced graphene oxide for methanol electro-oxidation*". Articles, 99, 998-1045
14. Mastrogostino M, Arbizzani C, Soavi F. (2001), "*Polymer-based supercapacitors*", Journal of Power Sources, 97-98, 812-815
15. Frackowiak E, Khomenko V. (2005). "*Supercapacitors based on conducting polymers/nanotubes composites.*" Journal of Power Sources, 15(20), 809-1147
16. Arrow Altech Distribution. (2012). "*High reliability EDLC supercapacitor ideal for extended temperature long-life applications*". Articles, 27, 56-119
17. Portet, C, Taberna, P. L, Simon, P, Flahaut, E, Laberty-Robert, C. (2012). "*High power density electrodes for Carbon supercapacitor applications*", Journal of Power Sources, 73, 88-369
18. Khomenko, V, Raymundo-Pinero, E, Frackowiak, E, Beguin, F. (2006). "*High-voltage assymmetric supercapacitors operating in aqueous electrolyte*". Applied Physics, A(82), 567-573
19. Dvořák P, (2010). "*Overview of non-aqueous electrolytes for supercapacitors*", Doctoral Degree Programme, (3)15, 16-98
20. Zhou Y, Narendran N. (2005). "*Photovoltaic-powered light-emitting diode lighting systems*", Optical Engineering (11)44, 1-6



21. Bonet F, Delmas V, Grugeon S, Urbina R. H, Silvert P-Y, Tekaia-Elhsissen K. (1999). "*Synthesis of monodisperse Au, Pt, Pd, Ru and Ir nanoparticles in ethylene glycol*". NanoStructured Materials, 11(8), 1277–1284
22. Sharma P, Bhatti T.S. (2010), "*A review on electrochemical double-layer capacitors*", Energy Conversion and Management 51, 2901–2912
23. Michio Inagaki, Hidetaka Konno, Osamu Tanaike. (2010), "*Carbon materials for electrochemical capacitors*", Journal of Power Sources 195, 7880–7903
24. Kotz, R. and M. Carlen (2000). "*Principles and applications of electrochemical capacitors*." Electrochimica Acta, 45(15-16), 2483-2498.
25. Endo M, Takeda T, Kim Y. J, Koshiba, Ishii K. (2001), "*High Power Electric Double Layer Capacitor (EDLC's); from Operating Principle to Pore Size Control in Advanced Activated Carbons*", Carbon Science, 1(3-4), 117-128
26. Frackowiak, E, Beguin F. (2001). "*Carbon materials for the electrochemical storage of energy in capacitors*." Carbon, 39(6), 937-950
27. Jayalakshmi M, Balasubramanian K. (2008). "*Simple capacitors to Supercapacitors – An overview*". International Journal of Electrochemical Sciences, (3)1196 – 1217
28. McAdams E. T, Lacknermeier A, McLaughlin J. A, Macken D. (1995). "*The linear and non-linear electrical properties of the electrode-electrolyte interface*", Biosensors and Bioelectronics. 10 (1–2), 67–74
29. Park S, An J, Piner R. D, Jung I, Yang D, Velamakanni A, Nguyen S. T, Ruoff R. S. (2008). "*Aqueous suspension and characterization of chemically modified graphene sheets*", Chemical Materials, 20, 6592-6594
30. Allen M. J, Tung V. C, Kaner R. B, (2009). "*Honeycomb carbon: A review of graphene*", Chemical Reviews, 73(15), 1190-2564

31. IOP Institute of Physics, “*Graphene: A new form of carbon with scientific impact and technological promise*”, <http://onnes.ph.man.ac.uk/nano>
32. Dreyer D. R, Park S, Bielawski C, Ruoff R. S. (2007). “*The chemistry of graphene oxide*”. *Chemical Society Reviews*, 56(11), 899-1045
33. Chen Da, Feng H, Li J, (2012). “*Graphene Oxide: Preparation, Functionalization, and Electrochemical Applications*”. *Chemical Reviews*, 112, 6027–6053
34. Ghosh A, Lee Y.H. (2012). “*Carbon-Based Electrochemical Capacitors*”. *ChemSusChem* 5, 480 – 499
35. Potts J. R, Lee S. H, Alam T. M, An J, Stoller M. D, Piner R. D, Ruoff R. S. (2011). “*Thermomechanical properties of chemically modified graphene/poly(methyl methacrylate) composites made by in situ polymerization*”. *Carbon*, 49, 2615–2623
36. Gómez-Navarro C, Burghard M, Kern K. (2008). “*Elastic properties of chemically derived single graphene sheets*”. *Nano Letters*, 8, 2045–2049
37. Chen Y, Zhang X., Yu P., Ma Y. (2009). “*Stable dispersions of graphene and highly conducting graphene films: A new approach to creating colloids of graphene monolayers*”. *Chemical Communications*, 45, 4527–4529.
38. Geim A. K, Novoselov K. S. (2007). “*The rise of graphene*”. *Nature Materials*, 6, 183–191
39. Stankovich S, Dikin D. A, Dommett G. H. B, Kohlhaas K. M, Zimney E. J, Stach E. A, Piner R. D, Nguyen S. T, Ruoff R. S. (2006). “*Graphene-based composite materials*”. *Nature*, 442, 282–286
40. Tjong S. C. (2012), “*Graphene and its derivatives: Novel materials for forming functional polymer nanocomposites*”. *Express Polymer Letters*, 6, 437 (2012).
41. Park S, Ruoff R. S. (2009). “*Chemical methods for the production of graphenes*”. *Nature Nanotechnology*, 4, 217–224 (2009).

42. Singh V, Joung D, Zhai L, Das S, Khondaker S. I, Seal S. (2011). “*Graphene based materials: Past, present and future*”. Progress in Materials Science 56: 1178–1271
43. Brownson D. A. C, Kampouris D. K, Banks C. E. (2011). “*An overview of graphene in energy production and storage applications*”. Journal of Power Sources 196, 4873–4885
44. Vivekchand S. R. C, Rout C. S, K S Subrahmanyam S. K. S, Govindaraj A, Rao C. N. R. (2008). “*Graphene-based electrochemical supercapacitors*”, Journal of Chemical Sciences”, 120(1), 9–13
45. Gudarzi M. M, Sharif F. (2012). “*Enhancement of dispersion and bonding of graphene-polymer through wet transfer of functionalized graphene oxide*”. Polymer Letters, 6(12), 1017–1031
46. Mishra A. K, Ramaprabhu S. (2011). “*Functionalized Graphene-Based Nanocomposites for Supercapacitor Application*”, The Journal of Physical Chemistry, 115, 14006–14013
47. Wilson N. R, Pandey P. I, Beanland R, Young R. J, Kinloch I. Gong L, Liu Z, Suenaga K, Rourke J. P, York S.J, Sloan J. (2012). “*Graphene Oxide: Structural Analysis and Application as a Highly Transparent Support for Electron Microscopy*”. American Chemical Society. 5(11), 775-889
48. Frackowiak E, Jurewicz K. (2001). “*Nanotubular materials for supercapacitors.*” Journal of Power Sources, 97(8), 822-825
49. Rao C. N. R, Subrahmanyam K. S, Matte H. S. S. R, Govindaraj A. (2012). “*Graphene: Synthesis, Functionalization and Properties*”, World Scientific Publishing, 12, 632-698



50. Shariahry L, Athawale A. A, (2014). “*Graphene Oxide Synthesized by using Modified Hummers Approach*”. Renewable Energy and Environmental Engineering, 02(01), 369-1478
51. Liang Z. X. (2013). “*Catalysts for Alcohol-Fuelled Direct Oxidation Fuel Cells*”. Platinum Metals Review, 57(4), 297–301
52. Grinou A, Yun Y.S, Cho S. Y, Park H. Y, Jin H-J. (2012). “*Dispersion of Pt Nanoparticle-Doped Reduced Graphene Oxide Using Aniline as a Stabilizer*”. Materials 5, 2927-2936.
53. Krehula S, Musiæ S. (2011). “*Hydrothermal synthesis of platinum group metal nanoparticles*”. Croatia Chemical Acta 84 (4) 465–468.
54. Rioux R. M, Songa H, Grassa M, Habasa S, Niesza K, Hoefelmeyera J. D, Yanga P, Somorjaia G. A, (2006). “*Monodisperse platinum nanoparticles of well-defined shape: synthesis, characterization, catalytic properties and future prospects*”. Topics in Catalysis, 39(3–4), 115-189
55. Nguyen V. L, Nguyen D. C, Hirata H, Ohtaki M, Hayakawa T, Nogami M. (2010). “*Chemical synthesis and characterization of palladium nanoparticles*”. Advanced Natural Sciences: Nanoscience Nanotechnology, 1(035012), 1-6
56. Shao G, Lu Y, Wu F, Yang C, Zeng F, Wu F. (2012). “*Graphene oxide: the mechanisms of oxidation and exfoliation*”, Journal of Materials Science, 47, 4400–4409
57. Rao C. R. K, Trivedi D, (2005), “*Chemical and electrochemical depositions of platinum group metals and their applications*”, Coordination Chemistry Reviews, 249, 613–631
58. Abragam A. (1968). “*Principles of Nuclear Magnetic Resonance*”, Cambridge University Press: Cambridge, 120, 115-987

59. Hafner B. (2012). *“Energy Dispersive Spectroscopy on the SEM: A Primer. Characterization Facility”*, University of Minnesota. 116, 89-198
60. Paulchamy B, Jaya J, (2015), *“A Simple Approach to Stepwise Synthesis of Graphene Oxide Nanomaterial”*, Journal of Nanomedicine and Nanotechnology, 6(1), 2157-7439
61. McGrail B. T, Rodier B, J, Pentzer E. (2014), *“Rapid functionalization of graphene oxide in water”*, Chemistry of Materials, 26(19), 5806-5811
62. Prasad K. R, Munichandraiah J, (2000). *“Platinum group metal nanoparticles”*. Journal of Power Sources 112, 443.
63. Ruas C. P, Fischer D. K, Gelesky M. A. (2013). *“PVP-Stabilized Palladium Nanoparticles in Silica as Effective Catalysts for Hydrogenation Reactions”*, Journal of Nanotechnology, 906740, 1-6
64. D.P. Dubal, D.S. Dhawale, R.R. Salunkhe, V.S. Jamdade, C.D. Lokhande, (2010), *“Fabrication of copper oxide multilayer nanosheets for supercapacitor application”*, Journal of Alloys and Compounds, 492, 26–30
65. Khomenko V, Frackowiak E, B´eguina F. (2005). *“Determination of the specific capacitance of conducting polymer/nanotubes composite electrodes using different cell configurations”*, Electrochimica Acta 50, 2499–2506